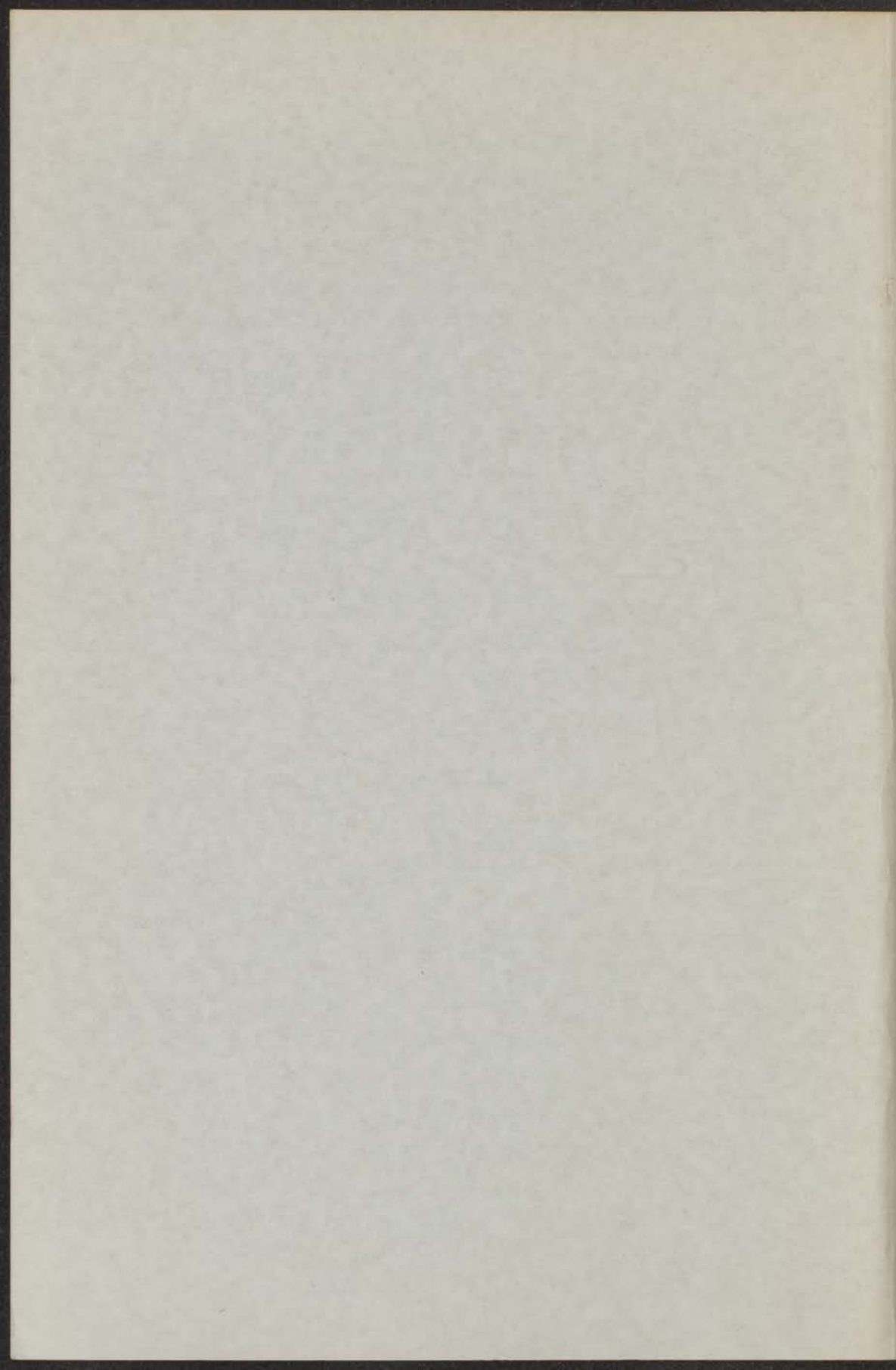


14C
51

THERMAL CONDUCTIVITIES OF SOME
NON-SUPERCONDUCTING ALLOYS AT
LOW TEMPERATURES

M. S. R. CHARI



THERMAL CONDUCTIVITIES OF SOME
NON-SUPERCONDUCTING ALLOYS AT
LOW TEMPERATURES

PROEFSCHRIFT

TER VERKRIJGING VAN DE GRAAD VAN
DOCTOR IN DE WIS- EN NATUURKUNDE
AAN DE RIJSUNIVERSITEIT TE LEIDEN, OP
GEZAG VAN DE RECTOR MAGNIFICUS
DR P. A. H. DE BOER, HOOGLERAAR IN DE
FACULTEIT DER GODGELEERDHEID, TEGEN
DE BEDENKINGEN VAN DE FACULTEIT DER
WIS- EN NATUURKUNDE
TE VERDEDIGEN OP
WOENSDAG 17 OCTOBER 1956
TE 16 UUR

DOOR

MADABHUSHI SRI RAMACHANDRA CHARI
GEBOREN TE GUNTUR (INDIA) IN 1917

THE THERMAL CONDUCTIVITIES OF SOME
NON-FERROUS METALS AND ALLOYS AT
LOW TEMPERATURES

PROPOSITION

Promotor: Prof. Dr. C. J. Gorter

RESEARCH REPORT NO. 10
OF THE PHYSICAL LABORATORY
OF THE TECHNICAL UNIVERSITY OF Delft

*To the memory of my father
To my mother
To my wife*

Presented by Prof. Dr. E. J. G. ...

To the memory of my father
To my mother
To my wife

Auto-biographical note, inserted at the instance of the Faculty of Mathematical and Physical Sciences.

Born in Guntur (South India), I had my early education at Guntur itself, first in the Town High School and later in the U.L.C.M. College. In 1935, I took the Bachelor of Sciences (B.Sc) degree of the Benares Hindu University with a first class and the first rank in the Mathematics, Physics and Chemistry group, and with a gold medal in Mathematics. A University Scholarship of Merit was awarded for post-graduate studies in the same University and I secured the Master of Science (M.Sc) degree in 1937, in the first class with first rank in Physics. I worked for some time on magne-crystallic action, under Prof. K. S. Krishnan D. Sc., F. R. S., at the Indian Association for the Cultivation of Science, Calcutta.

During the war, I served for a time at the R. A. F. Station, Santa Cruz (Bombay, India) as a civilian Meteorological Officer. I was then Commissioned as a Pilot Officer in the Meteorological branch of the Royal Indian Air Force (now, the Indian Air Force) and saw Active Service. Released with the rank of Flying Officer, I worked for a few years as a Lecturer in Physics.

In 1951, I joined the National Physical Laboratory of India. A Netherland Government Fellowship brought me to the Kamerlingh Onnes Laboratory, Leiden, in December 1953. I worked for some time with the Adiabatic Demagnetisation Group (under the leadership of Dr. M. J. Steenland) and participated in some of the investigations on Nuclear orientation.

The work described in the present thesis was done under the leadership of Dr. J. de Nobel and the over-all supervision of Prof. C. J. Gorter. It formed part of the research programme of the Netherlands 'Stichting voor Fundamenteel Onderzoek der Materie'. During the earlier part of the measurements, I had the co-operation of Mr. L. Kapel, while in the later part Miss J. Keyser gave valuable assistance. I had also the benefit of valuable discussions with Drs. A. R. de Vroomen. Mr. A. R. B. Gerritse did the glass-blowing work for us and Messrs D. de Jong and J. van Weesel gave useful technical assistance. Cryogenic technician A. Ouwkerk supplied the liquid Helium.

The Fellowship of the Netherlands Government terminated early in 1955, as did also the additional financial support given me by the Council of Scientific and Industrial Research, Government of India. From February 1955, I was given a research stipend by the "Netherlands Stichting voor Fundamenteel Onderzoek der Materie".

Contents

Chapter I.	Experimental details	9
§ 1.	Principle of the method	9
§ 2.	Apparatus used	13
§ 3.	The energy supply	16
§ 4.	The thermometry	18
	A. Making and mounting the thermometers	19
	B. Calibration procedure	22
	C. Behaviour of the thermometers	22
§ 5.	Sources of error	30
§ 6.	The Diesselhorst compensator	32
Chapter II.	Theoretical considerations	35
§ 1.	General survey of the theories of metals	35
	The Drude-Lorentz electron gas theory - Fermi-Dirac statistics - Sommerfeld free electron theory - Localised, molecular, and crystal orbitals - Bloch's work - Electron interaction theories	
§ 2.	Thermal conduction in non-metallic sub- stances	40
	Lattice vibrations and normal modes - Anharmonicity and Umklapp processes - Boundary scattering - Defect scattering	
§ 3.	Electronic thermal conduction in metals and alloys	45
	The Boltzmann equation - Electronic thermal resistivity W_e - The law of Wie- demann-Franz-Lorenz	
§ 4.	Lattice thermal conduction in metals and alloys	51
	Lattice thermal resistivity - Klemens' work - Choice of formula for λ_E	
Chapter III.	The Silver-base alloys	57
§ 1.	Introduction	57
§ 2.	Preparation of the alloys and determi- nation of solute concentration	58
§ 3.	The residual electrical resistivity	59
§ 4.	The electronic thermal resistivity	61
§ 5.	Discussion	61
	The λ vs T curves - The λ/T vs T curves - Interaction between phonons and elec- trons and the coupling between longitu- dinal and transverse phonons - The ap- plicability of Korringa-Gerritsen model to the present case	

Chapter IV.	The Steels	73
§ 1.	Introduction	73
§ 2.	The electrical and thermal resistivities	75
	The residual electrical resistivity - The thermal resistivity	
§ 3.	Discussion	79
	The λ vs T curves - The lattice thermal conductivity - The W-F-L parameter - Variation of λ with foreign metal con- tent - The λ/T vs T curves	
	List of important symbols used	89
	List of references	91
	Summary	95

Chapter I

Experimental details

§ 1. The principle of the method

The usual methods for thermal conductivity measurement consist in supplying a known amount of heat at one end of the experimental rod while its other end is maintained at a constant temperature; and then measuring the temperatures at intermediate points on the rod. They may be broadly distinguished as those based on a non-stationary temperature distribution and those based on a stationary distribution. In the former method, one measures the temperature as a function of time. This temperature variation with time would depend not only on the thermal conductivity of the specimen but also on its specific heat. Thus the quantity determined thereby, is the thermal diffusivity $D (= \lambda/\rho c$, where λ is the thermal conductivity defined as the heat flow per second across unit area of cross-section per unit temperature gradient, ρ is the density and c the specific heat) of the specimen. An independent determination of c is required before λ can be evaluated there-from.

We have found it more convenient to follow the second method in which a known amount of heat current Q (expressed in watts) is sent through the experimental specimen (which in all our experiments, is in the form of a uniform polycrystalline rod of circular or square cross-section), in the direction of the length axis. When the temperature distribution in the rod has attained equilibrium, the temperature gradient is measured by noting the indications of two thermometers T_1 and T_2 fixed at points A and B on the rod, 1 cms apart. Since equilibrium has been reached, the temperature distribution along the rod is now stationary - that is, independent of time; hence the name 'stationary distribution method'. Originally developed by *Lees* (1908), this method was successfully adapted to low temperatures, among others, by *De Haas* and his collaborators *Biermasz*, *Capel*, *Gerritsen* and *De Nobel*.

Let us set the origin of our rectangular co-ordinate system at A (see fig. I, 1) and consider the direction of heat-flow (in other words, the length axis of the rod) as the Y-axis. Remembering that λ is temperature-dependent, if we consider an arbitrary



Figure I,1

point P between A and B, at a temperature T and of ordinate y, we can write

$$Q = \lambda(T) \theta \frac{dT}{dy}$$

$$\text{or, } \int_0^l Q dy = Q l = \theta \int_{T_2}^{T_1} \lambda(T) dT \quad (I, 1)$$

where θ is the mean area of cross-section of the rod.

We might point out here that thermal conductivity is a tensor effect, the vector of density of heat flow being caused by the vector of temperature gradient. These two vectors need not necessarily coincide in direction, but since our material is homogeneous and isotropic, the tensor would reduce to a mere scalar quantity.

If we set the mean temperature between A and B as $\tau = \frac{T_1 + T_2}{2}$, and let $T - \tau = \varepsilon$, we can expand $\lambda(T)$ as a Taylor series, for evaluating the integral in equation (I,1) - compare Bremmer (1934) and De Nobel (1954).

Thus

$$\begin{aligned} \lambda(T) &= \lambda(\tau + \varepsilon) \\ &= \lambda(\tau) + \varepsilon \lambda'(\tau) + \frac{\varepsilon^2}{2!} \lambda''(\tau) + \dots \\ &= \lambda(\tau) + (T - \tau) \left(\frac{d\lambda}{dT} \right)_{\tau} + \frac{(T - \tau)^2}{2!} \left(\frac{d^2\lambda}{dT^2} \right)_{\tau} + \dots \quad (I, 2) \end{aligned}$$

where $\lambda'(\tau)$ and $\lambda''(\tau)$ are respectively, the first and second differential coefficients of λ with respect to temperature, at the mean temperature τ , and are thus written as $\left(\frac{d\lambda}{dT} \right)_{\tau}$ and $\left(\frac{d^2\lambda}{dT^2} \right)_{\tau}$. If λ can be considered a linear function of T, we need use only the first two terms in the series expansion (I,2). Thus

$$\int_{T_2}^{T_1} \lambda(T) dT = \left[\lambda_{\tau} T \right]_{T_2}^{T_1} + \left(\frac{d\lambda}{dT} \right)_{\tau} \left[\frac{(T - \tau)^2}{2!} \right]_{T_2}^{T_1} = \lambda_{\tau} \cdot (T_1 - T_2) ;$$

since the second term vanishes. Equation (I,1) can now be re-written,

$$Q = \frac{\theta}{l} \int_{T_2}^{T_1} \lambda(T) dT = \frac{\theta}{l} \lambda_{\tau} \cdot (T_1 - T_2) \quad (I, 3)$$

When, however, λ cannot be considered a linear function of T , we should include the third term as well from the expansion in (I,2), so that

$$Q = \frac{Q}{l} [\lambda_{\tau} \cdot (T_1 - T_2) + \frac{(T_1 - T_2)^3}{24} \left(\frac{d^2\lambda}{dT^2} \right)_{\tau}] \quad (I,4)$$

In such a case, we first assume a linear dependence of λ on T , evaluate λ_{τ} from equation (I,3), then obtain $(d^2\lambda/dT^2)_{\tau}$ and then recalculate the correct λ_{τ} , employing equation (I,4).

In the case of the alloys studied here, there was a slight departure of λ from linearity with respect to T , at liquid Helium temperatures. Since the heat current employed at these temperatures was rather small, it was considered necessary to estimate the effect of the term involving $(d^2\lambda/dT^2)$.

Taking, for example, the 1798H steel, the $(d\lambda/dT)$ versus T and $(d^2\lambda/dT^2)$ versus T curves were drawn and it was found that the largest value of $(d^2\lambda/dT^2)$, in the liquid Helium region amounted to 0.00035. For the corresponding measured point, $\Delta T = 0.147^\circ$, and since the form-factor $Q/l = 0.085$, the correction term $\left[\frac{Q}{l} \frac{(\Delta T)^3}{24} \left(\frac{d^2\lambda}{dT^2} \right)_{\tau} \right]$ amounted to $\approx 0.003 \mu\text{.watt}$. The value of Q actually used was 0.0486 m.watt, so that the correction term was negligible. For the rest of the steels, the correction term was even smaller in comparison with Q .

Taking the case of Ag-0.14%Mn, similarly, $(d^2\lambda/dT^2)$ amounted to 1.3, $Q/l = 0.0183$, $Q = 0.930 \text{ mW}$ and $\Delta T = 0.19^\circ\text{K}$, in the most unfavourable case. Thus the correction term was $2 \mu\text{W}$ in 0.930 mW, which was also negligibly small. For the other silver-base alloys the correction term amounted to even less.

In our further considerations, we shall therefore invariably employ equation (I,3) re-arranged in the form

$$\lambda_{\tau} = Q/l \cdot (T_1 - T_2) \quad (I,5)$$

It is evident from the fore-going discussion that i) all the power supplied Q should flow along the rod or, alternatively, stray heat losses should be taken into account, ii) $\Delta T = T_1 - T_2$ should be small compared to τ , in order to keep the last term in (I,4) low, in case λ_{τ} should vary rapidly with temperature, and

iii) ΔT should be measured accurately, as also Q , l and O . These requirements will be discussed at a later stage.

Since our rods are regular, having a circular or square cross-section, the mean value of O is easily obtained from a number of values measured between A and B . The distance AB ($= l$) should be rather large in comparison with the diameter of the rod, so that end-corrections become negligible. But this may lead to long equilibrium times, especially with the rather poorly conducting specimens. The thermometer T_2 is so attached that its distance from the bath is small compared to its distance from T_1 . If this condition is not satisfied, the temperature rises of both the thermometers would be large compared to ΔT , which is undesirable if only because it limits the lowest working temperature at which measurements can be made (Howling et al 1955).

For comparatively poor conductors like the stainless steel and the high nickel-content alloy-steels, it was found better to attach the heater (H) at the lower end-face (and not at a point on the side of the rod) and the thermometers to points A and B such that A and B lie on a line parallel to the length of the specimen. If these points are not kept in view, there would be only a very short length of specimen in which the temperature at all points in a cross-section would be the same (Berman et al 1953).

The quantities l and O are expressed in cms and cm^2 respectively. Since Q is produced electrically, it is convenient and conventional to express λ in watts/cm-deg. We will often be using the specific thermal resistance w (also referred to as the thermal resistivity) which is the reciprocal of λ and is expressed in $watt^{-1}\cdot cm\cdot deg$ (or $cm\cdot deg/watt$). This is related to the thermal resistance W of the specimen, by the equation

$$w = W O/l \quad (I, 6)$$

Introducing this latter in equation (I,5), we obtain

$$W = (T_1 - T_2)/Q, \quad \text{or} \quad Q = (T_1 - T_2)/W \quad (I, 7)$$

Equation (I,7) is the analogue of the well-known Ohm's Law, according to which the current strength in a conductor is proportional directly to the potential difference across its ends, and inversely as the resistance. There is this important distinction, however, that whereas the electrical resistance, under normal conditions, is independent of the potential, the thermal resistance is temperature-dependent. Thus, in investigating specimens

which have a marked variation of w with temperature, the temperature difference $T_1 - T_2$ (in other words, the power Q put in) should be kept reasonably small. We have mostly arranged to have $\Delta T < 1/10$ of τ , where τ is the mean temperature of the portion of the rod under investigation.

§ 2. Apparatus used

We will briefly describe the apparatus used by previous workers in this Laboratory, before taking up the apparatus used in the present investigations. In the apparatus developed by *De Haas* and *Bremmer* (1934) and adapted by *De Nobel* (1951, 1954) in some of his measurements, a gas thermometer and an electric heater were soldered at one end of the specimen under investigation, while the other end of the specimen was soldered to a brass plate, the latter being in direct contact with the bath liquid. The measured heat resistance evidently includes that of the solder and is therefore, too high. This is particularly so at low temperatures where the heat resistance of the solder, like that of other alloys, shows a marked increase.

The apparatus used by *De Haas* and *Biermasz* (1935) for material which could hardly or not at all be soldered, overcame this defect, and was also adapted by *De Nobel* (1951, 1954) in some of his measurements on hard steels, Aluminum, Dural etc. Since this apparatus had to be finally soldered with Wood's metal both at the top and the bottom seams, it had to be improved to serve for good conductors like Tungsten. Finally, a narrow bottom was incorporated for measurements in strong magnetic fields. Whereas

De Haas and *Bremmer* used a gas thermometer, two lead thermometers soldered at two points on the rod were used by the later workers. Heat energy was derived from a small electric heater soldered at the free end of the rod.

In our investigations with the stainless and the nickel steels, we used the apparatus indicated in fig. I,2. The experimental chamber comprised a brass cylindrical vessel *E* fitting tightly over the rim of the plate *C*, which was of thick copper in the original apparatus, but was later replaced by a thick

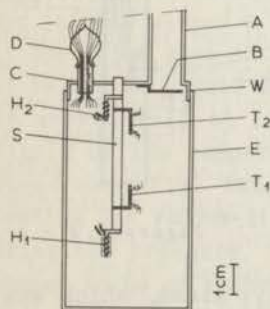


Figure I, 2

braas plate for obtaining a better Wood's solder joint between C and E. A platinum-glass seal D with ten platinum leads (insulated from one another by sheaths of glass fibre) served to convey the various electrical connections to the outside, while the german-silver tube A enabled the experimental space to be evacuated to under 10^{-6} mm of mercury. A radiation shield B, highly polished on the upper side, served to reflect back any radiations or hot gas molecules coming in through A. The specimen S was soft-soldered to C with its end protruding into the bath liquid, so as to have good thermal contact with the bath. The heater H_1 served to create the required temperature gradient between the points at which are soldered the thermometers T_1 and T_2 . By means of the heater H_2 , the entire rod S could be raised in temperature with respect to the bath.

For measurements on the silver-base alloys, the apparatus shown in fig. 1,3, was used, in which the important feature was that it had a very narrow stem, enabling measurements in very strong magnetic fields. In fact, the outer diameter of the bottom cap E was 15 mms, and since this was surrounded by two double-walled Dewar flasks, the outer diameter of the outer (liquid Nitrogen) Dewar was 40 mms. Correspondingly, the distance between the pole-pieces of the magnet was 42.5 mms, which gave about 1 mm space on either side, this being necessary in view of the pulling together of the pole-pieces when strong fields were used. The diameter of the pole-faces was 10 cms, so that the rods under investigation (which had a length of about 6 cms each and the distance between the thermometer contacts \approx 4 cms) could be arranged to lie in a reasonably uniform part of the magnetic field. A and D, as in the apparatus for the steels, indicate respectively the german-silver tube for evacuation and the platinum-glass seal. The platinum-glass seal, containing the platinum leads, was made out of Normal Jena 16_{III} glass, which was fused on to a platinum ring which was, in turn, soft-soldered to the apparatus. S is the specimen on which were mounted the heat-

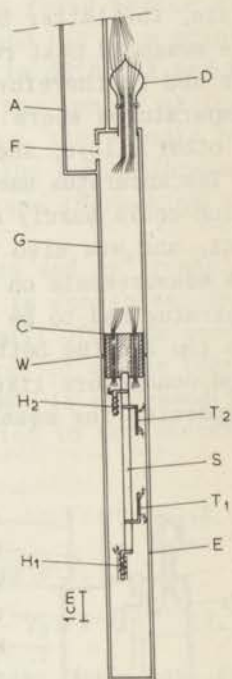


Figure I, 3

ers H_1 and H_2 and the thermometers T_1 and T_2 . C represents a thick copper block silver-soldered to the tube G. It had four narrow guide-holes (of about $2\frac{1}{2}$ mm diameter each) for the enamelled electrical leads which were further insulated from the body of the block by sheaths of glass fibre. These channels also served as vents for evacuating the space surrounding the specimen while, at the same time, they effectively prevented room temperature radiations or hot gas molecules from entering the space in E. The shape of the tube at F served a similar purpose.

To the under-side of C was soldered the sample S, so that good thermal contact was ensured between this end of the sample and the bath liquid. In the original form of the apparatus, E was of copper so that the Wood's metal solder joint at W was not quite satisfactory. It was therefore replaced by a brass cup which could be soldered better. In all thermal conductivity measurements, the space around the specimen was kept evacuated to below 10^{-6} mms of mercury by an Edwards oil diffusion pump and checked from time to time by a McLeod gauge.

At the top of the cryostat, there was a cap with four openings. Through one of these openings were led out the enamelled, double-silk covered copper leads (which had been plaited together and then coated with cellulose lacquer) by means of a glass-and-sealing-wax vacuum-tight seal. Another was for introducing the bath liquid and was closed down there-after, with a glass plug. The third led to the pump (for reducing pressure on the bath liquid), the manometer assembly and the regulating needle-valves. The fourth led to the high-vacuum pump and McLeod gauge, through a flat glass ground-joint.

Since it was essential to have the space surrounding the experimental rod evacuated to a good vacuum, the Wood's metal solder joint W played a vital role. It was sometimes found that even if the joint gave satisfactory vacuum at liquid air temperatures, it failed at liquid Hydrogen temperatures; and, at times, even if it served well at liquid Hydrogen temperatures, it failed at liquid Helium temperatures. For a perfect Wood's joint, it was found essential that the fit of the cap C on E was tight. In testing for vacuum-tightness, it was felt desirable, before measuring the pressure, to cut off the pumps (especially when they happen to be of rather high speed) by means of a stop-cock, suitably located. For making solder contacts on the experimental rods, pure tin was used, with a non-acid 'solfeen' flux. For stainless steel, a special flux 'nireosol' was used with soft solder.

The heater H_1 was made as follows: on a thick copper wire ($2\frac{1}{2}$ cm long and $1\frac{1}{2}$ mm diameter), coated with 'povine' varnish and well-baked there-after, was non-inductively wound fine enamelled constantan wire (0.05 mm diameter, and resistance per meter $\approx 260 \Omega$) in a single layer. A thin coating of yellow lacquer was given on the wire just at the moment of winding so as to have good thermal contact with the body of the heater (that is, with the thick copper wire). The winding was facilitated by observing under a binocular microscope at a magnification of about 15. The heat capacity of the heater body was thus ensured to be quite small. The heater was soft-soldered to the experimental rod at the bottom end-face and was covered with 'silver paper' in order to minimise heat loss by radiation. The heater H_2 was also wound in a similar manner, but since it had to take stronger current for raising the temperature of the specimen above that of the bath liquid, thicker constantan wire (diameter 0.10 mm, enamelled, and of resistance $\approx 66 \Omega$ per meter) had to be used, wound in layers.

The electric leads to the heaters and to the thermometers were thin enamelled constantan wires (diameter 0.10 mm and resistance $\approx 10 \Omega$) and these were soldered to the inner ends of the platinum wires of the seal D. By this means, heat leak to the bath through the leads was minimised. The outer ends of the platinum wires were connected to double-silk covered enamelled copper wires of about two meters length, coiled round the pumping tube A, thereby ensuring that they take up the temperature of the liquid in the bath and do not bring in heat from outside the cryostat, into the experimental space.

§ 3. The energy supply

In the stationary-flow method, a constant heat flow should be ensured and stray heat influx and out-flow through conduction, convection and radiation should be minimised and necessary corrections applied. In our measurements, the thermal energy was supplied (*Bremmer* 1934) by means of a small electric heater H_1 (fig. I, 4), soft-soldered at the bottom of the specimen. The electric current was derived from an accumulator battery C, connected through a potential divider, to the heater H_1 (wound from constantan wire and of resistance $\approx 400 \Omega$). A precision milliammeter A of Hartmann and Braun (having the ranges 3 and 15 ma for a scale of 150 divisions) measured i , the current in the main

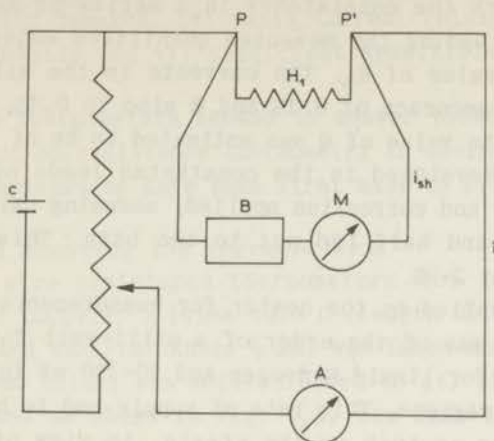


Figure I, 4

circuit. Another precision milli-ammeter *M* of Marek (Brémen) having the ranges 1, 3, 10 and 30 ma for 100 scale divisions, measured the current i_{sh} in the shunt circuit, comprising *M* and the precision decade resistance box *B* (of total resistance 11000 Ω) of Bleeker (Zeist, Holland). Absolute calibration was done for both the meters by a Diesselhorst compensator arrangement, employing a 'Zusatz' box and a standard Weston Cadmium cell. Calibration curves were prepared and corrections applied to the readings of the meters.

The resistance R_{sh} in the branch circuit comprised, besides the resistance set up in *B*, also the internal resistance of the milli-ammeter (for the particular range used) and the resistance of the leads joining *P* and *P'* respectively to *B* and *M*. The value of the resistance set up in the box *B* was almost always so chosen as to get as large a deflection in *M* as possible.

If i_h is the current in the heater proper and *V* the potential difference between the points *P* and *P'*, we have the relations

$$i_h = i - i_{sh} \quad (I, 8)$$

$$V = i_{sh} R_{sh} \quad (I, 9)$$

$$Q = i_h V \quad (I, 10)$$

We also calculated R_h , the resistance of the heater, from the relation

$$R_h = V/i_h \quad (I, 11)$$

This was to check the consistency in a series of measurements, any mistake in reading the measured quantities showing up immediately in the value of R_n . The currents in the milli-ammeters were read to an accuracy of 0.1% and R also to 0.1%, so that the uncertainty in the value of Q was estimated to be of the order of 0.5%. The heat developed in the constantan leads of the heater H_1 was evaluated and correction applied, assuming half of this to be led into H_1 and half led out to the bath. This correction amounted to about 2-3%.

The power supplied by the heater for measurements on the silver-base alloys was of the order of a milli-watt for the liquid Helium, 5-20 mW for liquid Hydrogen and 80-170 mW for the liquid Oxygen/Nitrogen regions. This rate of supply had to be drastically cut down when we took up the steels, in view of their much smaller thermal conductivities. The supply for the steels ranged between 0.03 to 0.2 mW for the liquid Helium region, 1-4 mW for the liquid Hydrogen and 10-60 mW for the liquid Oxygen/Nitrogen regions, - the lower limits being for the No.1798H steel and the upper for the 1287D steel. The purpose of the heater H_2 at the top of the experimental specimen was to enable the entire rod to be heated up to temperatures above the bath temperature. By this means, one could try to bridge the gaps between the liquid Helium and liquid Hydrogen, and between liquid Hydrogen and liquid Nitrogen temperatures.

§ 4. The thermometry

We did not use gas thermometry in spite of the advantages, namely, simplicity of calibration, suitability for measurement in the whole range upwards of 2°K even in a magnetic field, and adaptability to differential measurement. This was because one of the aims of this research was to develop resistance thermometry to replace the cumbersome gas thermometry. Further we could obtain a stronger magnetic field by using an apparatus having a very narrow stem. This would not have been possible with gas thermometers which need far more space around the specimen. Lastly, we could make measurements below 2°K without sacrificing accuracy. In designing the various thermometers used, the following points were kept in mind: i) lightness of weight and smallness of size, ii) possibility of using them over and over again

without losing reproducibility, iii) mounting in a manner so as not to be easily damaged, iv) small thermal relaxation times, v) small heat capacity and vi) sufficient sensitivity in the range meant for.

Resistance thermometers seemed to answer these requirements. The application of resistance thermometry to thermal conductivity measurements appears to have been first made by Lees (1908).

A. Making and mounting the thermometers:

a) The metal wire resistance thermometers (of platinum, phosphor-bronze or copper): A brass tube C (length $2\frac{1}{2}$ cms, outer diameter 5 mms, and wall-thickness $\frac{1}{2}$ mm) was taken and a copper wire AB (about $1\frac{1}{2}$ mm thick) was soft-soldered to it, the end A having been bent round as shown in fig. I,5, for ease in soldering to

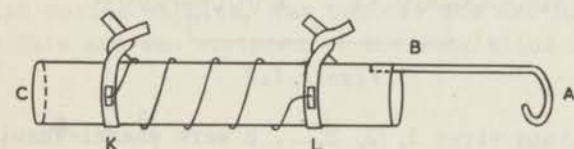


Figure I, 5

the experimental rod later. It was given a thin coating of povine varnish and subjected to the prescribed heat treatment. Two enamelled copper wires, K, L, each having a small length (on the side not in contact with the brass body C) stripped of the enamel insulation were wound once round, and fixed in position by a single twist, made rigid by a tiny drop of varnish. If the wire to be used for the thermometer was platinum, it was first suitably annealed, whereas if it were phosphor-bronze, it should be used in the springy state, since annealing renders its resistance in the Helium region, almost temperature-independent. One end of the wire was then carefully and well soft-soldered, as shown, to one of the spots, stripped of insulation. It was then moistened with just a trace of yellow lacquer and wound round the brass tube uniformly in a single layer, without short-circuiting adjacent windings. The other end of the wire was again soldered similarly to the clean spot on the other copper wire. A drop of varnish at each of these soldered joints was conducive to reduction of thermo-forces in the thermometer wire. At the ends of the copper wires K and L were soldered fine constantan wires (diameter 0.10 mm and resistance $\approx 10 \Omega$) to serve as the current and potential

leads, while at the same time minimising heat flow to the bath.

The thermometer wire should be wound tight without, in the least, straining or deforming it. This was rather difficult with the phosphor-bronze wire which had to be kept taut by attaching a suitable small weight at its free end, with wax.

'Combined thermometers' (comprising platinum for use at the higher and phosphor-bronze at the lower temperature ranges of the low temperature region) were also employed, with success. They were connected as shown in fig. I,6, for use with a Diesselhorst compensator, so that they could be used one pair at a time, as

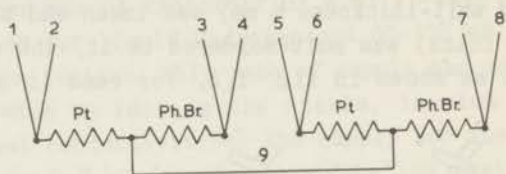


Figure I, 6

desired. The lead wires 1, 2, 3,... 8 were enamel-insulated thin constantan wires (diameter 0.10 mm and resistance $\approx 10 \Omega$) connected as shown, whilst their other extremities were soldered to the inner ends of the platinum wires of the platinum-glass seal. When the platinum thermometers were to be used, 1 and 5 formed the current leads while, when the phosphor-bronze thermometers were to be used, 3 and 7 were the current leads. In either case, 2, 4, 6 and 8 constituted the two pairs of potential leads. The wire 9 was of thin constantan (resistance $\approx 10 \Omega$ and diameter 0.10 mm) which gave a conduction path to electric current while, at the same time, minimising heat flow between the thermometers and their consequent equalisation of temperature.

It was essential to see that the varnish layer was not too thick for this would, for one thing, result in long relaxation times. Further, on cooling to low temperatures and warming up to room temperature, such a thick layer could crack and snap the thermometer wire. If, on the other hand, the varnish layer were not uniform, but in patches, there was the possibility of the thermometer wire getting electrically short-circuited to the brass body of the thermometer. In our experience, povine varnish served better than the usual 'glyptol' lacquer.

b) The Allen-Bradley carbon composition resistors:

Half-watt Allen-Bradleys (of nominal room temperature resis-

tance 56Ω) and deci-watt Allen-Bradleys (of nominal resistances 10 and 22Ω) were used by us. The plastic insulation was ground off in order to ensure optimum heat transfer. The resistor was then inserted into tightly fitting small copper jackets (length ≈ 6 mm and diameter ≈ 4 mm) which could later be soldered to the rod under investigation. A drop of glyptol lacquer (suitably thinned) was dropped in at either end of the carbon resistor, for better thermal contact with the copper jacket, and also to prevent possible adsorption of Helium gas by the carbon at the very low temperatures. The final soldering of the copper jacket to the experimental rod had to be done carefully lest the glyptol should melt and the thermometer should slip off the jacket.

c) Carbon film (*De Vroomen*) resistors *)

A piece of copper wire A (length ≈ 3 cm, diameter $1\frac{1}{2}$ mm) coated with povine varnish, was bent at the end D, as shown in fig. I,7. This end was stripped of its insulation and tinned so

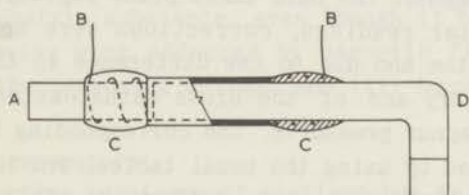


Figure I,7

that, after making the thermometer, it would be ready for soldering to the rod under investigation. Two short pieces of bare manganin or constantan wire were wound a few times round A at the points C, C, as shown, these points being a few millimeters apart. One end of each of these wires, B, B, was left free for making electrical connection. The points C were coated with silver paint (of E. I. Du Pont de Nemours and Co, Inc. U. S. A.) so as to completely cover the wire windings, and then allowed to dry for a short while at about 80°C . The alcohol-dag mixture was next coated in a uniform layer (the thickness of which decided the ultimate value of its resistance) and thoroughly dried for a few

*) We acknowledge indebtedness to Drs. A. R. de Vroomen of this laboratory for lending us some of his carbon resistors and for enabling us make such thermometers ourselves from his alco-dag mixture. This type of resistor was found very suitable for our research and will be referred to as the *De Vroomen* resistor.

hours in an electric oven at about 170°C, by which time the resistance attained a constant value. We found 1000 Ω a very suitable value for the nominal room temperature resistance.

B. The calibration procedure:

For obtaining the calibration points, the temperature of the bath was maintained constant by regulating the pressure above the bath liquid by controlling the pumping speed with the help of a needle-valve. To facilitate this adjustment, an oil differential manometer was used, the constancy of level where-in was an index of the constancy of the pressure. The pressure of the bath was read on a mercury manometer by a cathetometer, provided with a vernier which could read to 0.01 mm.

For temperatures above the λ -point of Helium, bath temperatures were always approached from above in order to avoid possible supercooling of the liquid below. Below the λ -point, in view of the high thermal conductivity of Helium II, temperature equalisation throughout the bath takes place rapidly.

To the manometer readings, corrections were applied due to capillary depression and due to the difference in thermal expansions of the mercury and of the brass cathetometer scale. From these corrected vapour pressures, the corresponding bath temperatures were obtained by using the usual tables. For Helium temperatures, the 1956 vapour pressure tables (*Van Dijk and Durieux 1955*) were used. For liquid Hydrogen temperatures were used tables prepared in this Laboratory on the basis of the formula of *Keesom, Bijl and Van der Horst (1931)*, namely

$$\theta = -260.865 + 1.0619 \log_{10} p + 1.7233 \log_{10}^2 p,$$

where θ is in degrees centigrade and p in cms of mercury. For Oxygen temperatures similar tables were used, prepared by Mr. *J.M.J. Koremans* of this Laboratory on the basis of the results of *Cath (1918)*. For Nitrogen temperatures, was used the formula, also due to *Cath*,

$$\log_{10} p = 7.781845 - 0.0062649 T - (341.619/T),$$

where p is in mm of mercury and T in degrees Kelvin.

C. Behaviour of the thermometers:

As metal wire thermometers, platinum, gold, constantan, manganin, lead, cadmium, phosphor-bronze etc. have been tried by

various workers for restricted temperature regions. No single wire material has been found capable of adequately covering the entire low temperature range. Since the electrical resistance of pure metals becomes practically independent of temperature in the region of liquid Helium temperatures (not taking the occurrence of super-conductivity into account), they are unsuitable for thermometry in that region. As regards thermo-elements, we need only make a passing reference: they are commonly used as thermometers at higher temperatures, but become less and less sensitive as we go to lower temperatures. Alloys like constantan and manganin, whose resistance at higher temperatures changes little with temperature, show some variation between 20 and 5°K. Yet they are not suitable for thermal conductivity measurements in view of their small dR/dT value per ohm, and their consequent inability to measure small temperature differences accurately enough. Lead turns superconducting at 7.2°K and is, besides, not easy to manipulate. Some specimens of phosphor-bronze serve very well as thermometric substance, even though it has the disadvantages of i) being much affected by magnetic fields, ii) being sensitive to the measuring current and iii) becoming insensitive above 10°K.

a) Platinum thermometers

We tried various specimens of platinum but we mention only one as an example. Very pure platinum wire of diameter 0.03 mm was softened in air by a current of 300 mA. It was then wound to serve as a thermometer in the manner already described. Using a measuring current of about 1/4 mA, its resistance was determined by comparing the potential drop across it, with that across a standard resistance by means of a Diesselhorst compensator, using a null method. The sensitivity was such that 2 mm on the galvanometer scale corresponded to 0.0001 Ω . On cooling from room temperature down to liquid air temperature, its resistance fell by a factor 5, while for cooling from there to liquid Hydrogen temperature, the resistance fell by a factor 35. In the Hydrogen region itself, the dR/dT per ohm dropped from about 0.2 to 0.1 as the temperature fell from 20° to about 15°K. Yet, for reasons to be given presently, it was not considered suitable for liquid Hydrogen temperatures.

b) Copper wire thermometers

Fine copper wire (diameter 0.03 mm and resistance 22 Ω /meter) showed a fall in resistance by a factor 7 when cooled from room

temperature down to liquid air temperature. In the liquid Nitrogen region itself, it showed an average dr/dT of 0.0284 per ohm. This was quite satisfactory. The fall in resistance on cooling from liquid air to liquid Hydrogen temperature was by a factor 8, while in the liquid Hydrogen region itself, the resistance variation was on the average 1/2 % per degree. Thus it was not suitable for use at liquid Hydrogen temperatures and therefore, on the whole, possessed no special advantage.

We would like to add a word of explanation here as to why platinum and copper were found not suitable for use at liquid Hydrogen temperatures. In the Diesselhorst compensator, we compare the potential drop E across the thermometer concerned, with that across a standard resistance. If R denotes the resistance of the thermometer, the rate of heat development in the thermometer during such a measurement would be E^2/R . In order to have less of this undesirable heat production in the thermometer, it is necessary to see that R does not fall too low. If we consider, for instance, the 0.03 mm diameter pure platinum wire, of room temperature resistance about 14 Ω , its resistance in the liquid Hydrogen region would fall to 0.08 Ω (in other words, one should start with about 175 Ω of such a wire at room temperature, in order to have 1 Ω resistance at liquid Hydrogen temperatures).

c) Phosphor-bronze thermometers

Keesom and *Van den Ende* (1929) found that a particular sample among a number of spools of phosphor-bronze wire supplied by Messrs. Hartmann and Braun, served very well as low temperature thermometer. Similar results for a sample of Hartmann-Braun phosphor-bronze were later reported by *Babbitt* and *Mendelssohn* (1935). Since the resistance-temperature curve began to show strong temperature-dependence near about 7°K, *Keesom* (1934) suggested that lead (whose transition temperature, in the pure condition, was known to be 7.2°K) was the substance responsible for this behaviour. This was confirmed by the observation that in large fields, the wire exhibited the more usual temperature-independent resistivity.

Keesom further postulated that the super-conducting inclusion (possibly lead or, may be, some super-conducting alloy) was in the form of thin needles parallel to the length of the wire. Moreover, since the needles were of random sizes, their super-conducting transitions would be spread over a temperature range so that, as the temperature fell, more and more needles became

super-conducting and thus caused the fall in resistance. The observation that annealing the wire rendered its resistance independent of temperature, was explained as being due to removal of the super-conducting inclusions whether by allowing these to go into homogeneous solution in the lattice, or by their evaporation at the surface.

Rather thick phosphor-bronze wires (diameter $\approx 100 \mu$) serve well in the upper liquid Helium range but exhibit a small dR/dT value in the lower liquid Helium range. The reverse holds for wires drawn to about 35μ diameter. We therefore put together two pieces of phosphor-bronze, one of 77μ and another of 48μ in series, to constitute a thermometer, so that it would show reasonable resistance variation over the entire liquid Helium region. Near about $4^\circ K$, its dR/dT was 0.0668 per ohm and at $1.5^\circ K$, it was 0.0634 per ohm. It could not, however, be used in the stronger magnetic fields, because it showed a temperature-independence even at $13 k\Phi$.

For the metal wire thermometers described above, calibration was done in the usual manner against the vapour pressure of the bath. Assuming a rectilinear relation $T = aR + b$, between the temperature T and resistance R of the thermometer, the constants a and b were evaluated from two of such calibration points. Knowing a and b , one could now calculate the temperature corresponding to the values of R measured at the remaining calibration points. A correction curve could now be drawn giving the correction which should be applied to any temperature indicated by this thermometer, in order to obtain the true temperature.

For instance, for two 0.01 mm diameter platinum wire thermometers A and B, we had the relations,

$$T_A = 2.50974 R_A - 7.6126$$

and
$$T_B = 2.03848 R_B - 6.1225,$$

at liquid Nitrogen temperatures. In the liquid Hydrogen region, the relations were

$$T_A = 15.2970 R_A - 225.16$$

and
$$T_B = 14.1777 R_B - 234.20,$$

in zero magnetic field, and

$$T_A = 15.5305 R_A - 228.85$$

and
$$T_B = 14.2273 R_B - 235.28,$$

in a magnetic field of 25 kΦ, on one and the same day. For two phosphor-bronze thermometers C and D of nominal room temperature resistance of 7 Ω (each thermometer comprising two wires, one of 77 μ thickness and another of 48 μ) we had similarly the following relations for the Helium temperatures, In zero magnetic field.

$$T_C = 3.66371 R_C - 9.82775$$

$$T_D = 4.43575 R_D - 0.25530$$

In a magnetic field of 5 kΦ,

$$T_C = 8.81650 R_C - 37.2195$$

$$T_D = 7.42444 R_D - 8.5370$$

In a field of 13 kΦ,

$$T_C = 319.713 R_C - 1461.325$$

$$T_D = -800.830 R_D + 1290.392$$

The calibrations were reproducible; but changed slightly from day to day, requiring calibration every time they were put to use. Provided the varnish layer was not too thick, the thermometers could be used repeatedly between room temperature and the lowest temperature they were meant for. If however the varnish layer was too thick, there was risk of the layer cracking (during these temperature cycles between room temperature and the very low temperatures), thereby straining and even snapping the fine wire.

d) Allen-Bradley carbon composition resistors

After a survey of the various commercially available composition radio resistors, *Clement and Quinnell* (1952) found the Allen-Bradley resistors to satisfy best the requirements of reproducibility and high sensitivity. For the liquid Hydrogen and Helium temperatures, they developed formulae of the type

$$\log_{10} R + \frac{A}{\log_{10} R} = B + \frac{C}{T},$$

where A, B, C, are determined from experiment. *Brown, Zemansky and Boorse* (1951) gave for ½ watt Allen-Bradleys, an equation of the form

$$\log_{10} R = A + BT^{-1} + CT^{-2} - DT^2$$

where A, B, C, D, are empirical constants. More recently *Worley, Zemansky* and *Boorse* (1954) suggested a relation of the type

$$\log_{10} R = A + \frac{B}{R} + C \log_{10} T + DT^4$$

for calibrating 1 watt and ½ watt Allen-Bradley resistors.

For using these resistors in the liquid Oxygen, Nitrogen and Hydrogen temperatures, the procedure was the same as with the metal wire thermometers. A rectilinear relation was assumed between temperature and the resistance of the thermometer. Rather than actually draw the T versus R straight line graph, we solved for the constants a and b of the equation $T = aR + b$, using two of the calibration points. The other calibration points would, no doubt, be slightly off this line. A correction curve of ΔT against T was drawn, T being the temperature indicated by the thermometer and ΔT the correction necessary to bring it to the value obtained from the vapour pressure of the bath.

For the Helium temperatures, we used the empirical formula evolved by *De Nobel* (1954), namely,

$$\log_{10} R - f = cT^{-1} + dT^{-\frac{1}{2}},$$

f, c, d being empirical constants. The inconvenience with the 56 Ω Allen-Bradley resistors used in the early stages of this research was that in the Helium region, the resistance rose from about 1300 Ω to about 146000 Ω . This high resistance created the risk of leakage by short-circuiting. Further, since we used a 2 volt accumulator in the measuring circuit, this meant a large fall in the measuring current. We therefore shunted a 10000 Ω resistance across the resistor, thereby making the effective resistance about 1100 Ω at the boiling point of Helium, rising to about 9400 Ω at the lowest Helium temperatures. The measuring currents used in the liquid Nitrogen, Hydrogen and Helium ranges were respectively 1/3 mA, 1/5 mA, and $\approx 15 \mu A$. The small size 10 Ω and 22 Ω Allen-Bradleys (Type TR, deci-watt) were more convenient in that their resistance did not reach such high values in the lower liquid Helium region. There was therefore no need to use 10000 Ω shunts across them. With the 10 Ω resistors, for instance, in the liquid Nitrogen, Hydrogen and Helium regions, we used measuring currents of 2/3 mA, 1/4 mA and 50 μA respectively, so that the rate of heat generation in the thermometers in these temperature ranges were of the order of 5 μW , 1 μW and 1/2 μW .

In the presence of a magnetic field, their resistance showed a

rise ΔR which, for a given temperature was the larger, the higher the field; and for a given field, ΔR was the larger the lower the temperature. At the highest magnetic field used by us, namely 25 k Φ , the value of $\Delta R/R_{H=0}$ for the 22 Ω resistors for instance, was about 1% at 4°K, 2% at 2.5°K and 5% at 1.2°K. Further, $\Delta R/R_{H=0}$ departed considerably from proportionality to the square of the field strength.

e) The de Vroomen carbon film resistors

As prepared from an aqua-dag mixture, these resistors, which were of a nominal room temperature resistance of 490 Ω showed a resistance increase of 14%, 25-35% and 200-340% respectively in the liquid Nitrogen, Hydrogen and Helium regions. A second aqua-dag mixture was then prepared which gave much better sensitivity and was mainly used in our measurements. As compared to the room temperature resistance of 1000 Ω , these resistors increased in resistance at the liquid Nitrogen, Hydrogen and Helium temperatures respectively 1.25, 1.9-2.1, and 3.5-9 times. These were used with a Wheatstone bridge, the currents sent through them in the liquid Nitrogen, Hydrogen and Helium temperature regions being respectively of the order of 40 μA , 15 μA and 4 μA , and the corresponding amounts of heat generated per second in the resistor 2 μW , 1/2 μW and 1/10 μW .

In a magnetic field, the resistance invariably diminished so that $\Delta R = (R_H - R_{H=0})$ was negative, whereas it was positive in the case of the Allen-Bradleys. At the highest field strength used by us, namely 25 k Φ , the numerical value of $\Delta R/R_{H=0}$ was about 1/4% at 1.2°K, rising steeply to about 1% near about 4°K, diminishing gradually there-after and reaching about 3/4% at liquid Hydrogen temperatures.

We painted these resistors with a thin protective coating of yellow lacquer, and then their change in nominal resistance from day to day was insignificant even after thermal cycles between room temperature and Helium temperatures. If however, they were removed from a particular specimen and again soldered on to another, they did show a rise in nominal resistance, which again stayed reasonably constant at the new value. This rise may be due to slight mechanical strains introduced in the process of transfer from one specimen to another. Calibration of these thermometers was done every measuring day at 6-8 points and separate calibration curves prepared. Random checks at the end of the measuring day showed no deviation from the calibrations done at the beginning of the day. If measurements were to be done in

magnetic fields, calibration was also done in these fields at each of the zero-field calibration points and separate calibration curves drawn for each value of magnetic field employed.

We found the behaviour of the de Vroomen resistors with regard to temperature as well as to magnetic fields, perfectly reproducible and independent of current strength in the range of currents used by us. As with the Allen-Bradleys, a higher nominal room temperature resistance gave at low temperatures, a higher resistance and also a high (negative) temperature coefficient of resistance. For this reason, in measurements at liquid Nitrogen and liquid Oxygen temperatures, we preferred de Vroomen resistors of a nominal room temperature resistance of about 2000 Ω .

For measuring the resistance of the carbon resistors, we used a conventional Wheatstone bridge circuit. The ratio arm comprised two oil-immersed manganin resistances, wound non-inductively on bakelite formers and having nominal resistances 100 Ω and 1000 Ω respectively, By means of a two-way switch, one could bring into the bridge circuit, either of the resistors with its corresponding balancing decade boxes. The voltage employed to drive current through the bridge was arranged to be 0.3 V, 0.5 V and 1 V respectively for the liquid Helium, Hydrogen and Nitrogen temperature regions. The galvanometer used was a double-coil Kipp Kc galvanometer (of P. J. Kipp and sons, Delft, Holland), having a voltage sensitivity of 0.2 to 2.0 μV for 1 mm deflection on a scale 1 meter off.

Imperfectly soldered joints and switches making imperfect contacts could give rise to annoying thermo-forces. By using soft easy-flowing solder with a non-acid "solfeen" flux, by carefully choosing our switches and by employing an enclosed-mercury double commutator, we successfully minimised these thermo-forces.

Since the major part of our investigation was done using the sensitive de Vroomen resistors, it may not be out of place to give an idea of the attainable accuracy of these. We take as example a 1500 Ω resistor.

1) Liquid Nitrogen temperatures: Using a current of 40 μA , a variation in resistance of 0.05 Ω would give rise to a difference of potential of 2 μV , which was well within the range of sensitivity of our galvanometer. Since in this temperature region, the resistor had a resistance variation of 7.5 Ω per degree, we could, by measuring the resistance to five-hundredths of an ohm, obtain temperatures correct to better than 0.01°K. Since ΔT was

chosen to be about 2°K at these temperatures, this could give an accuracy of $1/2\%$ in ΔT .

ii) Liquid Hydrogen temperatures: The temperature coefficient of resistance in this range was between $50\ \Omega/\text{degree}$ (at 20°K) and $100\ \Omega/\text{degree}$ (at 14.5°K) so that by measuring the resistance to a tenth of an ohm, one could read temperature differences to an accuracy of about 2 milli-degrees. Since ΔT was of the order of 0.5°K in this region, one could reach an accuracy of about $1/2\%$.

iii) Liquid Helium temperatures: The temperature coefficient of the resistors in this region was about $1000\ \Omega/\text{degree}$ (at 4°K rising rapidly to about $10000\ \Omega/\text{degree}$ at 1.5°K) so that measuring resistance to the nearest ohm gave ΔT to the nearest milli-degree. Since ΔT was chosen to be 0.2°K , the accuracy in ΔT was $1/2\%$, improving considerably in the liquid Helium II region.

§ 5. Sources of error

Since the heat resistance is given by $\Delta T/Q$, we should consider the sources of error in the measurement of ΔT and Q . Errors in the measurement of the power supplied Q could be due to the following sources:

i) Heat developed in the thermometers: As explained already in subsection 'e' of the section on thermometry, the rate of heat generation in the thermometers was of the order of $1/10\ \mu\text{W}$ at the lowest temperatures, whereas the power supplied Q was at least a fraction of a milli-watt for the silver-base alloys and at least $30\ \mu\text{W}$ for the steels. Thus the effect of this heat development in the thermometers, on the value of Q , was negligibly small at the Helium temperatures, and formed an even smaller fraction at the higher temperatures, in view of larger values of Q at those temperatures. The heat led out from the thermometers to the bath was likewise small since the heat resistance between the thermometers and the bath via the constantan leads amounted to much more than $10^7\ \text{cm. deg/watt}$.

ii) Heat developed in the lead wires of the heater H_1 : We always used thin constantan leads of about $10\ \Omega$ resistance, for this purpose. The amount of heat developed in these leads and the amount led away to the bath along these leads are not precisely known. Their thermal resistance, however, amounted to more than $10^7\ \text{cm. deg/watt}$, whereas the experimental rod had a thermal resistance, orders of magnitude smaller - the worst case being the

1798H steel rod at the lowest liquid Helium temperatures, where the heat resistance amounted to 9000 cm-deg/watt. It was therefore permissible to assume that half the heat developed in these constantan leads was led away to the bath, the other half being led to the heater. A correction was accordingly applied which amounted at most to 2-3% of the value of Q .

iii) Room temperature radiations and 'hot gas' molecules entering from the upper part of the cryostat: We have already discussed how this was minimised in our apparatus.

iv) The heat lost through the residual gas molecules in the vacuum space surrounding the specimen: As was done by *Schott* (1916) and earlier by *Meissner* (1914), we always evacuated the space to less than 10^{-6} mm of mercury, so that heat transmission by conduction and convection would be negligibly small. Radiations from the heater to the walls of the surrounding vessel would arise if there is a large thermal resistance between the heater wire and the metal body on which it is wound, resulting in the heater wire being considerably heated up. We took the further precaution of covering the heater with 'silver' paper.

The heat-loss by radiation from the experimental rod itself, to the surrounding walls was also estimated, assuming the rod to be a perfectly black body. Even in this limit, the correction needed to Q at liquid Nitrogen temperatures, amounted to less than 0.1% in the case of the silver-base alloys and about 0.8% for the worst conducting no. 3754 steel. At lower temperatures, these corrections became negligible.

v) The determination of Q itself was done from the readings of two carefully-calibrated sensitive milli-ammeters, and the resistance of the heater evaluated each time, as an indirect check against incidental 'slips' in observation and transcription.

Sources of error in the measurement of ΔT were as follows:

i) Heat developed in the thermometers themselves on account of the measuring current flowing through them: As already explained, the effect of this was negligibly small.

iii) The possible accuracy in the measurement of ΔT , using the de Vroomen resistors has already been discussed. In practice, such high accuracy could not be attained since there seemed no sufficiently accurate method of converting the resistance changes into temperature differences. At liquid Nitrogen and Hydrogen temperatures, a plot of $\log R$ of each of the thermometers against T , on a large graph sheet, gave a reasonably good method. The inaccuracy in reading temperatures therefrom, could amount to as

much as 0.01°K in the liquid Nitrogen and 0.005°K in the liquid Hydrogen temperature region. For the liquid Helium temperatures, this method could be elaborated by dividing the region into two sub-regions (with a small overlap for counter-check) and drawing separate $\log R$ versus T calibration curves for the two thermometers.

It was however felt that the use of two independent calibration curves was not conducive to an accurate determination of ΔT . The following method was therefore developed, which was also useful for obtaining ΔT at intermediate temperatures, meaning those lying between liquid Helium and liquid Hydrogen, or between liquid Hydrogen and liquid Nitrogen temperatures.

This method was based on the fact that for any two de Vroomen thermometers chosen at random from a crop, the resistance variation with temperature was similar. We accordingly plotted R_A/R_B against R_B , from the calibration points of that day. A smooth curve generally resulted, but any slight deviation of one or more of the calibration points was automatically corrected by the smoothening. When thermal energy was supplied, resulting in a temperature gradient along the rod, the temperature of the A-thermometer (denoted by T_A) was directly read from a calibration graph of $\log R_A$ against T . The measured resistance of the B-thermometer was referred to the R_A/R_B versus R_B graph, wherefrom one obtained the value R'_A which was the resistance the A-thermometer would register if it were at the same temperature as the B-thermometer. The value of the temperature corresponding to this R'_A was again read from the calibration curve, $\log R_A$ versus T . In this manner, we obtained ΔT using the calibration curve of one thermometer (here, the A-thermometer), while the calibration of the other thermometer gave us the auxiliary curve of R_A/R_B versus R_B .

§ 6. The Diesselhorst compensator

We used a five-decade Otto Wolffe compensator. Figs. I.8 and I.9 show how the thermometers were connected for measurement of their resistance. We might add here that the compensator was used only for measurements with the metal wire thermometers and the small Allen-Bradleys, whereas the Wheatstone bridge was employed with the de Vroomen resistors. The figures are self-explanatory and the principle of the Diesselhorst compensator too well-known to need much comment.

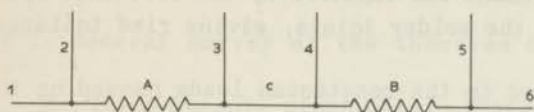


Figure I, 8

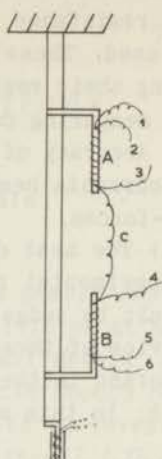


Figure I, 9

"c" was a piece of thin constantan wire (0.10 mm diameter, $\approx 10 \Omega$ resistance), enamelled and double-silk covered, which brought the two thermometers into the same measuring circuit while at the same time, preventing them from equalising in temperature. This was possible since the thermal resistance of such a piece of constantan wire amounted to more than 10^7 cm-degrees per watt. The oil-immersed standard resistance N (of 10Ω , 1Ω , or 0.1Ω , as necessary) and the thermometers A and B were connected, in series, in the same measuring circuit. By means of a selector switch, one could connect the potential terminals of N (or A or B, at will), to the terminals on the compensator, marked X. The decade contacts of the compensator were adjusted until the galvanometer gave zero deflection. The reading on the decades was at once seen to be a measure of the resistance, whose terminal potential difference was applied at X. This was because the adjustment of the knobs of the decades no way affected the current in the compensation circuit.

We used the Diesselhorst compensator, also for measuring the electrical resistances of our rod specimens whose thermal conductivity was under investigation. The straight-forward method would be to measure the electrical resistance simultaneously with the thermal resistance measurement, thereby ensuring the same form-factor. However, since for the latter measurement, the rod had to be in the vacuum space, the following considerations rendered electrical resistance measurement under the same circumstances, inconvenient:

i) Since the rods were rather thick and were of very low electrical resistance, fairly strong electric currents ($\approx \frac{1}{2}$ Amp) had to be used. These currents heated up the constantan leads, increasing their resistance, which again resulted in a gradual fall of the measuring current.

ii) Accuracy of measurement was impaired by the fact that such large currents heated up the solder joints, giving rise to large thermo-forces.

iii) The heat developed in the constantan leads passed on to the experimental rod, raising its temperature. This rendered it difficult to judge the actual temperature of the rod.

In view of these considerations, the rods were mounted directly immersed in the bath liquid, and the constantan leads dispensed with. In this manner, thermo-forces were eliminated entirely.

Chapter II

Theoretical considerations

§ 1. General survey of the theories of metals

The *Drude-Lorentz* electron-gas theory:

Wiedemann and *Franz*, in 1853, postulated on purely empirical grounds, that the electrical and thermal resistivities at a given temperature, should bear a constant ratio for all metals. *Lorentz* went further, in 1872, indicating that this ratio should be proportional to the Absolute temperature. Attempts to investigate the mechanism of metallic conduction came only after *J.J.Thomson's* discovery (1897) of the electron. *Drude* (1900) started with the assumption that the electrons in a metal were not bound to specified positions but were free to move subject only to resistive forces. With this 'electron gas' conception of a metal, he succeeded in giving a theoretical basis to the formulations of *Wiedemann*, *Franz*, and *Lorentz*. He obtained for the *Lorentz* parameter, defined as $\lambda/\sigma T$, the value $3(k/e)^2$. Considering the crudeness of the model, this value is in excellent conformity with experiment. *H.A.Lorentz*, in 1905, improved the theory employing the *Maxwell-Boltzmann* statistics and scrutinizing the collision-dynamics. The *Drude-Lorentz* theory enabled a simple derivation of the well-known *Ohm's* law and threw light on the high-frequency optical properties of metals, which latter was vindicated by the infra-red optical studies of thin metal films by *Hagen* and *Rubens*. This simple theory, however, led to a specific heat contribution of $3k/2$ per electron, whereas experiments on specific heats of metals showed no such contribution.

Fermi-Dirac statistics:

Pauli, in 1925, enunciated the famous Exclusion Principle which required that only one electron could occupy a quantum state specified by four quantum numbers, three spatial and one of spin. In 1926, *Fermi* and *Dirac* independently worked out the statistical behaviour of independently moving particles subject to the *Pauli* principle. The classical *Maxwell-Boltzmann* statistics served for the low particle densities obtaining in gases under ordinary conditions, and when applied to electrons in a metal,

permitted of any number of them having identical energy and momentum. In the Fermi-Dirac quantum statistics, which reduces to the Maxwell-Boltzmann type for low particle densities, the probability for a quantum state of energy ϵ to be occupied is given by the function f ,

$$f = \left[\exp \left(\frac{\epsilon - \zeta}{kT} \right) + 1 \right]^{-1} \quad (\text{II, 1})$$

where ζ is a parameter which equals the maximum energy of the Fermi surface. It is seen from the form of equation (II, 1) that the Fermi energy ζ has the significance of a cut-off energy at the Absolute zero of temperature, all states with a lower energy being completely filled and those with a higher energy lying vacant. The Fermi energy, therefore, indicates the top of the filled energy levels, being fixed by the condition that the filled levels contain just as many electrons as are actually known to be present. When the temperature is raised above 0°K , some of the states slightly below the Fermi level will be depopulated and the electrons from them raised to levels slightly above the Fermi level.

The *Sommerfeld* 'free electron' theory:

The incorporation of the Pauli principle and the Fermi-Dirac statistics into the discussion of transport phenomena in metals was achieved by *Sommerfeld* in 1928. In this model, the electrons are considered free (that is, without mutual interaction) within the boundaries of the specimen, and the effect of the crystal lattice is ignored. To put it more precisely, the positive charge is assumed distributed uniformly throughout the crystal, so that the electrical potential is constant in the metal, increasing to another constant value at the boundary. Whilst the electronic specific heat, in classical statistics, should be constant, *Sommerfeld* showed, with the aid of Fermi-Dirac statistics, that for a degenerate electron gas, it should be proportional to T and have a value much less than the classical value. This removed one of the main lacunae in the Drude-Lorentz theory; but probably the most important contribution of the *Sommerfeld* theory is that it showed a free electron to be not necessarily a conduction electron.

For the electrical and thermal conductivities σ and λ , *Sommerfeld* obtained the equations,

$$\sigma = (8\pi/3)^{1/3} (e^2 l/h) n^{2/3} \quad (\text{II, 2})$$

and

$$\lambda = (8\pi/3)^{1/3} (\pi^2 k^2 Tl/3h) n^{2/3} \quad (\text{II, 3})$$

where l stands for the electronic mean free path and n for the number of free electrons per unit volume. One of the main shortcomings of the theory was that it offered no *a priori* basis for evaluating or even estimating the value of l . Thus the absolute values of σ and λ could not be obtained. However, by taking their ratio, one obtained

$$\begin{aligned} \lambda/\sigma T &= \frac{\pi^2}{3} \left(\frac{k}{e}\right)^2 & (\text{II, 4}) \\ &= 2.7 \times 10^{-13} \text{ e. s. u./deg}^2 \\ &= 2.45 \times 10^{-8} \text{ watt-ohm/deg}^2 \end{aligned}$$

This value agreed with experimental results and, being independent of the metal, vindicated the Wiedemann-Franz-Lorenz law.

In the later theories of electronic conduction in metals, the statistical properties of free electrons were combined with the motion appropriate to an electron moving in an electric field having a periodic potential.

Localised, Molecular and Crystal orbitals:

Soon after the introduction of wave mechanics, attempts were made to set up self-consistent fields for atomic systems. *Hartree* (1928) framed equations, where-in the potential function was the Coulomb potential due to the fixed ion cores together with that of the rest of the electrons in the system. There were two distinct approaches to solving such equations. In the *Heitler-London* (1927) scheme of 'localised orbitals', each electron wave function was localised and was large near to only one ion core in the crystal. In the other approach, the electron wave function was assumed to extend over the entire system, so as to have equal probability density at equivalent atoms. The latter approach was used by *Hund*, *Mulliken* and *Lennard-Jones* in the elucidation of the structure of di-atomic and poly-atomic molecules (- the method of 'molecular orbitals'), and by *Bloch* (in his work on 'crystal orbitals'), *Peierls*, *Bethe*, *Sommerfeld*, *Wilson*, *Brillouin*, *Wigner* and *Seitz* among others, in the discussion of the solid state.

In the application of wave mechanics to the discussion of molecule formation, it was soon realised that an electron in a wave function shared by two atoms (- the so-called symmetric wave function) could result in their binding together, whereas an

electron in an anti-symmetric type of wave function gave rise to repulsion. Such wave functions came to be referred to as 'molecular orbitals', the former as the 'bonding orbital' and the latter as the 'anti-bonding orbital'. When one considered two isolated atoms gradually brought nearer to each other to form a diatomic molecule, each energy level of the individual atoms was split into two levels. The lower level corresponded to a bonding orbital having the charge distribution concentrated between the atoms while the upper corresponded to an anti-bonding orbital, the electrons avoiding the mid-points between the atoms.

The problem of an array of atoms in a crystal lattice was just an extension of this picture. Energy levels were now more or less continuously distributed between the lower and the upper energy limits. In other words, each energy level of a free atom gave rise to a continuous band of energies, the so-called 'energy band'. The major contribution to the energy band picture was that of *Bloch* and it was further developed by *Brillouin*, *Kronig*, *Penney* and numerous other investigators, incorporating the concept of Brillouin zones in momentum space.

For the computation of wave functions in metals, the 'cellular' method introduced by *Wigner* and *Seitz*, and extended by *Slater* and by *Bardeen*, has also come to the fore-front. In this model, the lattice is divided up into space-filling polyhedra, the so-called 'cells', each of which is centred round an atom of the metal.

Bloch's work:

Bloch (1928) showed with complete generality, that in a perfect crystal lattice, wherein the potential is exactly repeated at intervals of the lattice constant, the crystal orbital solution (the *Bloch* function) to the one-electron Schrodinger equation, leads to the electron waves behaving as progressive or stationary waves whose amplitude has the same periodicity as the lattice potential. One important deduction from this is that these 'Bloch waves' traverse a perfect crystal without diminution in energy. Secondly, each electron in the crystal is characterised by a velocity vector, for certain values of which correspond regions of forbidden energy. If the permitted vectors are plotted in three-dimensional space (the \mathbf{k} space), the end point of each vector indicates a possible electronic state for the system.

The first deduction throws new light on the aspect of electrical resistance. Whereas in the classical electron theories,

collisions between electrons and atoms led to a finite free path and a consequent resistance to the electron stream, wave mechanics requires that a perfect single crystal of a pure metallic element, at the absolute zero of temperature, should exhibit no electrical resistance, unless the electron wave happened to have the correct wave-length and direction for a *Bragg* reflection. Resistance is caused, firstly, by interaction with the elastic Debye waves representing thermal vibrations (see § 2), that is, by the scattering of electrons by the atoms which are displaced from their equilibrium positions in the lattice during their thermal motion. This comprises the 'ideal temperature-dependent part of the resistance. Secondly, resistance is also caused by chemical impurities in the form of foreign atoms, and by physical lattice defects, both of which act as scattering centres and give rise to the temperature-independent (the so-called 'residual') part of the resistance. The empirical *Matthiessen* rule (1864) thus obtains theoretical support.

In considering how the periodicity of the lattice potential affects the energy distribution of the electron gas, two approaches are possible. In the 'tight-binding' (or 'nearly bound' electron) approximation, the electron energies and wave functions are taken the same as when associated with a free atom, and the lattice periodic potential is brought in as a perturbation to treat the ions constituted into a crystal. In other words, the electron wave functions are built up out of the atomic wave functions surrounding the ions of the lattice. When the wave functions of adjacent ions overlap, the discrete atomic levels spread out into energy bands in the crystal, the width of the band depending on the extent of overlap.

In the 'weak-binding' (or 'nearly free' electron) approximation, the energy of a free electron is taken over from the electron gas model, and the periodic lattice potential applied as a small perturbation. Here also the energy gaps appear at certain critical values of the electronic wave numbers, and these values correspond to electron waves which suffer selective reflection from the crystal planes in accordance with the *Bragg* condition for X-ray reflection. From a general consideration of electron propagation in periodic structures, *Brillouin* showed that the energy bands comprise all levels for which the wave vectors lie within certain definite polyhedra in \mathbf{k} space, the energy cut-off values forming the edge of a so-called Brillouin Zone in \mathbf{k} space.

The concept of allowed and forbidden bands, in other words, the functioning of the lattice as a low-pass filter on the electron waves bears analogy to lines of electric filters displaying pass-band and cut-off properties, or to acoustic systems filtering high-frequency waves.

Electron interaction theories:

The theories discussed so far are basically one-electron (or the 'independent electron') theories which ignore interactions between the electrons. In developing the collective description of electron interactions, analogy has been drawn between the electrons in a metal and the free ions in an ionised gas (the so-called 'plasma') by *Kronig and Korringa* (1943, 1949) and worked out in detail by *Bohm and Pines* (1951, 1952, 1953, 1954). A plasma could also be looked upon as an electron gas in a uniform back-ground of positive charge, except that typical plasma densities are of the order of $10^{12}/\text{cc}$, whilst metallic electron densities are of the order $10^{23}/\text{cc}$.

§ 2. Thermal conduction in non-metallic substances:

Lattice vibrations and Normal modes

In the simple approach of *Boltzmann* to the aspect of internal energy of solid bodies, every atom in the body had a position of rest, about which it executed thermo-kinetic oscillations. As a first approximation, the force binding the atom to its equilibrium position was assumed 'elastic' (that is, proportional to the displacement of the atom) which caused the atom to execute harmonic vibrations at constant frequency. In reality, the atoms constituting a crystal are rather bound to one another forming a coupled system. In such a case, as shown by more advanced mechanics, 'normal co-ordinates' could be introduced which are linear combinations of the co-ordinates of the atoms comprising the system. For a crystal containing N atoms, there are in all $3N$ co-ordinates, each of the normal co-ordinates being a linear combination of all these $3N$ co-ordinates; and the total number of the normal co-ordinates is also $3N$.

Each of the normal co-ordinates can vibrate independently of the others, with its own frequency, giving rise to a normal mode of vibration. If atoms of equal mass be present in the lattice, this normal vibration is an ordinary sound wave which may be considered as a stationary wave or as a progressive wave, according

to convenience. There are in all, $3N$ normal modes, and in the general type of motion, all these modes are superposed, each having its own frequency, amplitude and phase. The total vibrational energy of the lattice is the sum of the energies of these normal modes, each of which according to the Quantum theory, amounts to $\frac{1}{2} h\nu + \frac{h\nu}{\exp(h\nu/kT) - 1}$. The first term in this expres-

sion is the zero-point energy (that is, the energy retained by the oscillator at Absolute zero of temperature) and the second, the temperature-dependent component of energy which tends to zero as T tends to 0°K . As the temperature is gradually raised starting from 0°K , it can be seen that the energy is associated mainly with the lowest frequencies in the beginning, while at higher temperatures, the higher frequencies are excited and contribute to the thermal energy.

The above conceptions are due to *Debye* who looked upon a solid as an elastic continuum, whose frequency spectrum is cut off at a limiting frequency ν_D (the Debye frequency). The quantity defined by $\theta_D = h\nu_D/k$, is called the Debye temperature of the substance. The low frequency normal modes can be assigned a wave vector, for each value of which three independent normal modes are possible, corresponding to the three directions of polarisation,

Peierls applied Quantum mechanics to the aspect of the energy content of a normal mode. Instead of saying that an oscillator (of wave vector \underline{q} and of polarisation \underline{s}) is excited to its n 'th state, we now say there are n quanta of vibration of wave vector \underline{q} and of polarisation \underline{s} . Such quanta which bear to sound waves the same relation as do photons to light waves, are referred to as 'phonons'. It is seen that an assembly of phonons obeys *Bose-Einstein* statistics.

Anharmonicity and Umklapp processes:

In non-metallic substances or di-electric solids, heat transport is through the lattice waves, - the phonons. For a perfect crystal with harmonic inter-atomic forces (the potential energy is a quadratic function of relative displacements), the normal modes are progressive plane elastic waves, each lattice wave being independent of the others, leading to an infinite free path and infinite thermal conductivity. In actual crystals, deviations of the lattice from perfect periodicity and harmonicity obtain, the elastic potential energy contains also terms of higher power of the amplitudes, and plane waves are no longer the normal

modes. Thus results mutual scattering and attenuation of the waves and consequently, a heat resistance. This was first recognised by *Debye* (1914) but the modern theory of heat conduction in di-electric solids may be said to originate from the rigorous mathematical formulation by *Peierls* (1929), who treated the solid as a lattice. Considering the solid as elastically isotropic, further extensions of *Peierls*' picture have been attempted, but the treatment by *Klemens* (1951) is probably one of the most satisfactory.

In the presence of a constant temperature gradient, the total momentum of the 'phonon gas' down the temperature gradient continuously increases, whilst processes which scatter the phonons try to efface the excess momentum. The resultant heat current is determined by the phonon distribution, which is obtainable by solving the *Boltzmann* integro-differential equation.

In a large crystal without impurities, structural defects, strains etc., anharmonicity of interatomic forces causes inter-phonon collisions, and is the only scattering agency. For temperatures rather smaller than θ_D , *Pomeranchuk* (1941a, b, 1942) showed that there are very few collisions which alter simultaneously the occupation numbers of four or more normal modes. *Peierls* (1929, 1935) showed further that only three-phonon collisions are of importance, wherein two phonons coalesce to form a third, or vice versa. The 'ordinary' or 'momentum-conserving' three-phonon processes satisfy the equations

$$\omega_1 + \omega_2 = \omega_3 \quad (\text{II, 5})$$

and

$$\underline{q}_1 + \underline{q}_2 = \underline{q}_3 \quad (\text{II, 6})$$

corresponding to the laws of energy and momentum conservation. Since the energy carried by the phonons is unaltered by the collision (equation II,5), and the direction of energy flow is also unchanged (equation II,6), these ordinary three-phonon collisions do not explicitly find a place in the expression for thermal resistivity. Yet they do have an indirect influence in that they can change the polarisation of the phonons, rendering them more susceptible to other scattering processes.

Peierls also showed that for a discrete lattice, there are 'Umklapp' processes which obey the equations

$$\omega_1 + \omega_2 = \omega_3 \quad (\text{II, 5})$$

$$\underline{q}_1 + \underline{q}_2 = \underline{q}_3 + 2\pi \underline{b} \quad (\text{II, 7})$$

where \mathbf{b} is a reciprocal lattice vector. Though energy is conserved in these processes and there is some degree of correlation between the initial and final directions of energy flow (as indicated by equation II,7) in as much as \mathbf{b} can have any one of six directions parallel to the crystal axes (for simplicity, *Peierls* treats a cubic lattice), the result is much the same as if the phonons are randomly scattered. Thus they contribute to heat resistance.

It was shown further by *Peierls* (1929) that for temperatures above θ_D , the umklapp resistivity (also called the intrinsic thermal resistivity) is proportional to T , whilst at low temperatures, $\omega_U \propto T^{-2} \cdot \exp(-\theta_D/2T)$.

Boundary scattering:

In real crystals, thermal conductivity is limited not only by U-processes but by all phonon-scattering processes which do not conserve momentum. These other processes are i) scattering at external boundaries, grain boundaries and by mosaic structure and ii) elastic and inelastic scattering by static impurities and imperfections such as strains, faults in periodicity and dislocations.

In deriving the normal modes of a crystal, it is assumed that the displacements at the crystal boundaries are periodic, whereas the actual boundary is far more complex. This gives rise to scattering which has been extensively studied by *De Haas* and *Biermasz* (1935, 1937). Since this is one of the scattering processes for which the absolute value could be reasonably estimated, *Casimir* (1938) worked out the consequences of *Peierls*' suggestion that crystal boundary scattering should become important at low temperatures. *Casimir* took the analogy of the flow of radiation down a cylindrical tube having diffusely reflecting walls. Ignoring phonon interactions except at the external boundary, where the phonons are assumed to be absorbed and re-emitted isotropically, he showed that the thermal conductivity becomes size-dependent and is no longer an intrinsic property of the material.

Casimir's result is $\lambda_B = 2.31 \times 10^3 R p A^{2/3} T^3$ watts/cm-deg, where the dimensionless quantity p has the value 1.4 for most crystals, R is the radius, A is the constant in the expression $c_v = AT^3$ for the specific heat per unit volume at low temperatures on the Debye theory. For a crystal of square cross-section having side 'a', $R = 0.56 a$. We will express the thermal resistivity due to boundary scattering as

$$w_B = B/T^3 \quad (\text{II}, 9)$$

B being the phonon-boundary scattering coefficient. *Berman, Simon and Ziman* (1953) made detailed study of boundary scattering and showed that 'specular' (in contrast with 'diffuse') reflections at the external boundary increase the phonon mean free path. They also calculated the reduction in mean free path for a rod of finite length.

Expressing λ_B in the Debye form

$$\lambda_B = l c_v u/3 \quad (\text{II}, 10)$$

where c_v is the specific heat per unit volume, l the mean free path and u the phonon group velocity (= velocity of sound), it can be shown that l is of the order of the shortest linear dimension of the crystal. *Pomeranchuk* (1942) had indicated that the scattering at a small-angle grain boundary should be as the square of the frequency, so that the thermal resistivity should be proportional to T^{-1} : (this can be easily derived from equation II,10, remembering that u can be regarded nearly independent of T , and that for temperatures $T < \theta/10$, c_v can be taken to be proportional to T^3). *Klemens* (1955) has shown, however, that at low frequencies ($< 1/6$ of the limiting frequency ν_D), the *Pomeranchuk* type of scattering which arises from the disordered region immediately adjoining the grain boundary contributes only a fraction of the total scattering probability, the major part being due to the strain field at large distances. Thus (*Klemens*, 1956) there exists no difference in principle, between scattering at a small-angle grain or mosaic boundary in a crystal and that at a crystallite boundary in a polycrystalline solid, - except that the scattering probability of the former is smaller.

Defect scattering:

Pomeranchuk (1942) showed that inelastic scattering by defects can be neglected. *Klemens* (1951) has worked out the Quantum Mechanical theory of elastic scattering of phonons by static imperfections of atomic dimensions. An impurity can be expected to perturb the lattice potential on account of i) the difference between the masses of the solvent and the solute atoms and ii) the difference between the elastic properties of the solvent-solvent and solvent-solute atomic linkages. At low temperatures, where only small wave numbers are present, *Klemens* neglects dispersion and calculates the scattering probability using the terms

in the perturbation energy which are quadratic in the phonon amplitudes (this is because only these terms describe elastic scattering). He then finds that the scattering probability is proportional to (frequency)⁴, so that the heat resistivity arising on this account, is given by

$$w_D = DT \quad (\text{II, 11})$$

The coefficient D on the right hand side of this equation is the phonon-defect scattering coefficient. *Klemens* finds also no essential difference between the scattering powers of vacancies and substitutional impurities. For single dislocations, in view of their long-range strain field, he obtains a scattering probability proportional to frequency, so that

$$w_d = d/T^2 \quad (\text{II, 12})$$

where d is the phonon-dislocation scattering coefficient.

For the over-all lattice thermal resistivity of a dielectric solid, we can write

$$1/\lambda_g = w_g = w_B + w_D + w_d + w_U \quad (\text{II, 13})$$

to a satisfactory approximation. (The use of the sub-script 'g' for lattice conductivity has its origin in the German word 'Gitter'). Actually, if τ be the effective relaxation time and τ_α the relaxation time for the individual scattering process indicated by the index α , then $1/\tau = \sum_{\alpha} 1/\tau_\alpha$, this additivity relation being

applicable to each individual frequency. *Klemens* (1951) has shown that under conditions when two of these scattering terms are of comparable magnitudes, the total w_g is larger than given by equation (II.13).

§ 3. Electronic thermal conduction in metals and alloys

The *Boltzmann* equation:

In metallic substances, heat can be transported not only by the phonons but also by the conduction electrons, the latter process being dominant in pure metals. Even for specimens containing upto 0.1% impurity (see for instance, *Hulm*, 1950), $\lambda_g \ll \lambda_e$, where λ_e is the electronic thermal conductivity. We will now consider λ_e , λ_g being taken up in § 4. We confine ourselves to

polycrystalline metals, assuming them to behave like isotropic media.

The evaluation of λ_e involves, as does also the evaluation of σ , the determination of the distribution function of the conduction electrons in the presence of an external field. Since the heat flow due to a constant temperature gradient is defined under conditions when there is no electric current, a slight re-distribution of the electrons is necessary, for creating an appropriate electric field which would counteract the electronic drift caused by the temperature gradient. The evaluation of the velocity distribution function is then based on the *Boltzmann* integral equation,

$$\mathbf{v}_x \frac{\partial f}{\partial \mathbf{x}} + \frac{e\mathbf{X}}{\hbar} \frac{\partial f}{\partial \mathbf{k}} = [\partial f / \partial t]_{\text{coll}}$$

$$\text{or,} \quad \mathbf{v}_x \frac{\partial f}{\partial T} \frac{\partial T}{\partial \mathbf{x}} + \frac{e\mathbf{X}}{\hbar} \frac{\partial f}{\partial \mathbf{k}} = [\partial f / \partial t]_{\text{coll}} \quad (\text{II, 14})$$

in which the direction of temperature gradient is chosen as the x -axis, X is the x -component of the electric field referred to above, $-e$ is the electronic charge, \mathbf{v} is the electronic velocity and f the distribution function. The terms on the left hand side of the equation are proportional to the change in distribution caused respectively by the electronic motion with velocity \mathbf{v}_x , and by the field X acting on the charge. The term on the right hand side gives the change in distribution due to the various scattering (collision) mechanisms.

The solution of this equation has so far been carried out only for quasi-free electrons, for which $\epsilon = \hbar^2 \mathbf{k}^2 / 2m$. For certain types of scattering mechanisms, it turns out that $[\partial f / \partial t]_{\text{coll}}$ can be written in the form

$$[\partial f / \partial t]_{\text{coll}} = - \frac{f - f_0}{\tau} \quad (\text{II, 15})$$

where f_0 and f are the distribution functions, under equilibrium and in the presence of the temperature gradient. In other words, when a non-equilibrium distribution function f is set up by a system of external forces and these forces are suddenly removed, the rate of approach to equilibrium distribution f_0 , under the influence of these collisions is given by equation II, 15. The problem is then comparatively simplified but, in general, the

solution is complicated. Assuming a relaxation time, the Boltzmann equation can be written thus:

$$\mathbf{v}_x \frac{\partial f}{\partial T} \frac{\partial T}{\partial \mathbf{x}} + \frac{e\mathbf{X}}{\hbar} \frac{\partial f}{\partial \mathbf{k}} = - \frac{f - f_0}{\tau} \quad (\text{II, 16})$$

As evaluated from this equation, the expressions for electrical and thermal conductivities σ and λ involve integrals containing f_0 which can be evaluated to any desired order, for temperatures $T \ll \zeta/k$. The first term in the expansion turns out to be the only important one in the case of σ , whereas in the case of λ , this term vanishes identically and second order terms are to be used. For this reason, thermal conductivity is referred to as a 'second order' effect.

For cubic and isotropic metals, the conductivities are:

$$\sigma = \frac{e^2}{12 \pi^3} \int \frac{\tau v^2 dS}{|\text{grad}_{\mathbf{k}} E|} \quad (\text{II, 17})$$

and

$$\lambda = \frac{k^2 T}{36 \pi} \int \frac{\tau v^2 dS}{|\text{grad}_{\mathbf{k}} E|} \quad (\text{II, 18})$$

where \mathbf{v} is the electron velocity ($= \frac{1}{\hbar} \frac{d\epsilon}{d\mathbf{k}}$), k is the Boltzmann constant and dS an element of the *Fermi* surface. The integrations are over the Fermi surface ($\epsilon = \zeta$). If in these two equations, the τ 's are the same (that is, τ is independent of the deviation of the distribution from equilibrium), we obtain the electronic Lorenz parameter L_e to be

$$L_e = \lambda/\sigma T = \pi^2 k^2 / 3e^2 \quad (\text{II, 19})$$

which becomes independent of relaxation time and of the band structure. This value of L_e is due to the assumption of degeneracy of the electron gas.

Electronic thermal resistivity, w_e :

Wilson showed (*Theory of Metals*, 1936) that the electronic thermal resistivity of metals can be expressed as the sum of two components (in analogy with *Matthiessen's* rule for electrical resistivity) caused by the scattering of the conduction electrons respectively by the impurities (or static imperfections such as strains, displaced atoms etc.) and by phonons. Thus

$$w_e = w_0 + w_i \quad (\text{II, 20})$$

w_0 is the 'impurity' or 'residual' thermal resistivity and is connected with the 'residual' electrical resistivity ρ_0 by the relation

$$\rho_0/w_0T = L_0 = \pi^2 k^2/3e^2 \quad (\text{II, 21})$$

L_0 being the 'ordinary' (or 'normal') Lorenz parameter. w_i is characteristic of the metal and is called the 'ideal' thermal resistivity (sometimes referred to as the 'intrinsic' thermal resistivity).

In order to obtain w_i , the electron-phonon interactions are regarded as processes in which an electron and a phonon of wave vectors respectively \underline{k}_1 and \underline{q} interact resulting in an electron wave vector \underline{k}_2 (compare the three-phonon processes of § 2), or vice versa, satisfying the energy conservation condition

$$\epsilon_1 + \hbar\omega = \epsilon_2 \quad (\text{II, 22})$$

and $\underline{k}_1 + \underline{q} = \underline{k}_2 \quad (\text{II, 23a})$

or $\underline{k}_1 + \underline{q} = \underline{k}_2 + 2\pi\mathbf{b} \quad (\text{II, 23b})$

the last refers to Umklapp processes, wherein an electron suffers simultaneously a favourable phonon collision (that is, absorption of an energy quantum), which elevates it to the Brillouin zone boundary, where it then incurs momentum reversal by Bragg reflection (by being strongly diffracted by the lattice).

The theory of Bloch (1928, 1930) for the case of electrical resistance, starts with a spherical Fermi surface, ignores Umklapp processes and assumes the phonons to have a distribution characteristic of true thermal equilibrium despite deviations of the electron distribution from equilibrium. Wilson (1937) and Makinson (1938) took over Bloch's picture (including the assumption that only longitudinal phonons can directly interact with the electrons) and discussed the case of thermal resistance. They obtained for w_i at low temperatures, the equation

$$w_i = \alpha T^2 \quad (\text{II, 24})$$

where

$$\alpha = \frac{A}{\lambda_\infty \theta^2} N_a^{2/3} \quad (\text{II, 25})$$

N_a is the number of conduction electrons per atom, λ_∞ the limiting thermal conductivity at high temperatures, and A is a dimensionless constant. Bremner (1934) obtained $A = 27$, whereas Wilson,

employing a variational method due to *Kroll* (1933) and *Kohler* (1948, 1949), obtained at a first approximation, the value 95.3 for *A. Sondheimer's* (1950) third approximation gave $A = 71.6$, while *Klemens* (1954a), solving numerically the appropriate transport equation for low temperatures, obtained $A = 64.0$.

If N_a be evaluated from equation (II, 25), it is found (*Hulm*, 1950) that N_a is about 0.02 even for metals for which one would normally expect N_a to be about 1. Similarly for Tungsten single crystals, *De Nobel* (1954) found N_a about 0.2. Further the additivity of w_o and w_i expressed by equation (II, 20) has been shown by *Sondheimer's* (1950) third approximation to be not strictly valid. The measurements of *White* (1953 a, b, c) on copper, silver and gold also seem to indicate this departure from strict additivity of w_o and w_i . The correction terms are however not large and for all practical purposes, the following equation for electronic thermal resistivity is taken as valid:

$$w_e = w_o + w_i = \beta T^{-1} + \alpha T^2 \quad (\text{II, 26})$$

where $\beta = \rho_o/L_o$ (II, 27)

In a pure metal, lattice thermal conduction is negligible compared to electronic thermal conduction, so that the behaviour of the thermal conductivity of a metal will be as given by equation (II, 26). The impurity term β/T obtains only at the lowest temperatures, so that as the temperature rises, w_e falls in inverse proportion. A minimum of w_e is reached at a temperature T of the order $\theta/10$ or lower, and then the ideal resistivity term takes hold and w_e begins to increase (rather sharply in the case of pure metals, especially those having a low Debye θ). This increase becomes less steep at higher temperatures. In the presence of even a small impurity, w_e is increased and the w_o term becomes dominant over a wider temperature range, so that the w_e versus T curve, instead of presenting a minimum, continues to be inversely proportional to T , for a considerable temperature range. In an alloy (wherein we have several per cent of solute atoms), w_e is very much increased and λ_e diminished until it is of the same order as λ_g . The behaviour of the total thermal conductivity of an alloy is therefore much different from that of a pure metal.

The law of Wiedemann-Franz-Lorenz:

In discussing thermal and electrical conductivity data, we are often confronted with the question as to the validity of the

W-F-L law. Since this law connects electrical and thermal resistivities, it can evidently be expected to hold as long as the mechanism causing these resistivities is one and the same.

Looking at the Quantum Mechanical view of the electrical resistance mechanism, when the electric field is applied, the momenta of the electrons in the partially filled Brillouin zones begin to grow with time. After a short while, there will be an excess of electron momentum down the field direction. In other words, there is an electric current, and this process should continue and the current keep growing unless there is some mechanism which tends to obliterate the excess electronic momentum in the direction of the field. Phonons and impurities (or irregularities) afford the scattering mechanisms whereby the electrons can make quantum transitions to other vacant states, so that the electron wave vector shifts into a different direction. In momentum space, this would correspond to a movement of the electrons from one side of the Fermi surface to the opposite side (- the so-called 'horizontal' movement: see *Klemens* 1954c, 1956; *Fröhlich* 1936). At low temperatures, the electron scattering angle is small being of the order T/θ , so that the resistance mechanism consists in a slow diffusion of the electrons along the Fermi surface. We might add here that the electrical resistance, on this account, would depend on the actual configuration of the Fermi surface, - that is, whether the surface is spherical, whether it touches a zone boundary, etc.

The thermal resistivity, on the other hand, can be due to i) elastic collisional processes (which change the direction of the electron wave vector, keeping the electron energy unchanged) which are due to collisions with imperfections and impurity atoms, and cause the 'horizontal' movement (referred to in the previous paragraph) along the Fermi surface, and ii) inelastic collisional processes (which change the energy by an amount of the order kT) which are due to electron-phonon collisions, and cause the so-called 'vertical' movement on the Fermi surface. In the latter process, as distinguished from the former, the electron movement is from a point just above the Fermi surface to a point just below, or vice versa. The scattering corresponding to this would evidently be independent of the shape of the Fermi surface.

We thus see that the electrical resistance mechanism (which, as has been shown above, is characterised by 'horizontal' move-

ment) and the 'horizontal' thermal resistance mechanism are processes giving identical relaxation times, and therefore the W-F-L law should hold good under these circumstances. In other words, as long as the thermal resistivity is dictated by impurity scattering, this law should be valid for all temperatures. This enables us to determine λ_e from the constant electrical residual resistance ρ_o , using the W-F-L law thus:

$$\rho_o / w_o T = L_o, \quad \text{or} \quad w_o = \rho_o / L_o T \quad (\text{II, 28})$$

$$w_e = w_o + w_i \simeq w_o \quad (\text{II, 29})$$

since $w_i \ll w_o$, when the resistance is purely residual. Thus,

$$\lambda_e = 1/w_e \simeq 1/w_o = L_o T / \rho_o \quad (\text{II, 30})$$

Even when the electron scattering is inelastic (when, for instance, the electrons are scattered by the phonons), we see that if $T \gg \theta$, the change in electron energy due to impact with a phonon will be $k\theta$, which is small compared to kT . Thus, for such temperatures, the electron-phonon collisions may be considered roughly elastic, and the W-F-L law can be expected to be obeyed.

Wilson (1937), *Sondheimer* (1950) and *Makinson* (1938) have discussed the theoretical behaviour of the electronic Lorenz parameter $L_e = \lambda_e / \sigma T$, with respect to temperature and the purity of the metal. For monovalent metals at high and low temperatures, L_e should approach the 'ordinary' value L_o , whilst for an ideally pure metal, L_e should tend to zero as T tends to 0°K . For intermediate temperatures, L_e should fall below the 'ordinary' value, this fall being less for greater impurity. For metals containing small number of free electrons (like bismuth), the behaviour at high and at low temperatures would not be much different, but at intermediate temperatures, L_e should rise to a maximum above L_o , and with lowering of temperature, fall to a minimum below L_o .

§ 4. Lattice thermal conduction in metals and alloys

The lattice thermal resistivity, w_g :

The presence of conduction electrons in metallic substances, while constituting a medium for heat conduction, forms also an extra scattering mechanism for the momentum transfer of the phonons. This brings down the lattice thermal conductivity. Yet, in the case of metals or alloys which have a small λ_e , the λ_g may

be comparable to λ_e . It was first pointed out by *Köningsberger* (1907) that the heat transport by electrons and by the lattice could be taken as independent processes wherefore one could express the total thermal conductivity λ as

$$\lambda = \lambda_e + \lambda_g \quad (\text{II, 31})$$

For obtaining the lattice thermal resistivity w_g , we can extend the theory of thermal conduction in dielectric solids (discussed in § 2) to the present case, considering the phonon+electron interaction as an additional scattering mechanism causing a resistivity w_E . We can thus write, for the over-all lattice thermal resistivity w_g ,

$$w_g = w_B + w_E + w_D + w_d + w_U \quad (\text{II, 32})$$

The scattering of phonons by electrons can be treated as has been done for scattering of electrons by phonons (see § 3) assuming i) a spherical Fermi surface, ii) the electron distribution function to have the equilibrium value, iii) U-processes to be negligible and, of course, iv) the possibility of direct interaction between the phonons and the conduction electrons. *Bethe* (1933) worked out the relaxation time for this scattering process assuming, like *Bloch*, that transverse phonons cannot directly interact with conduction electrons. On the other hand, assuming phonons of all three polarisations to interact equally with the conduction electrons, *Makinson* (1938) has shown that where electron interactions play a dominant role in limiting the phonon free paths, the lattice thermal conductivity λ_E is given by

$$\lambda_E = 1/w_E = \frac{8 \pi^2 P \theta^2 k^3 M}{h^3 a^3 C_L^2} \left(\frac{T}{\theta}\right)^2 \left(\frac{1}{k} \frac{d\varepsilon}{dk}\right)^2 \zeta \quad (\text{II, 33})$$

where θ is the Debye temperature, M the atomic mass, 'a' the lattice constant, ε and k are the energy and wave number of an electron state, C_L (which has the dimensions of energy) is the constant of interaction between the conduction electrons and the longitudinal phonons. The constant P has a value of about 7.18 for temperatures $T \ll \theta$. We will write, for short,

$$w_E = E/T^2 \quad \text{or} \quad E = w_E T^2 \quad (\text{II, 34})$$

E being the phonon+electron scattering coefficient. But we have seen that the component of lattice thermal resistivity (w_d) caused by the scattering of phonons by single dislocations has

also the same temperature dependence as w_E (Klemens 1955), and we know no way of separating the effects of these two processes, by purely thermal conductivity measurements. We will henceforth write, for the over-all lattice thermal resistivity w_g ,

$$w_g = w_B + w_E + w_D + w_U \quad (\text{II, 35})$$

bearing in mind that the term w_E and the corresponding scattering coefficient E include the effect of dislocations as well.

Klemens' work:

Makinson assumed that all modes of polarisation interact equally with the conduction electrons. The constant C_L in equation (II, 33) is therefore related to the interaction constant C in the full expression for electronic thermal conductivity λ_e , by the equation, $C_L^2 = \frac{1}{3} C^2$. Since, however, the actual value of C_L is not known, *Makinson* (1938) expressed λ_E for a free-electron gas in terms of $\lambda_{i(\infty)}$, the ideal electronic thermal conductivity at high temperatures. Thus

$$\begin{aligned} \lambda_E &= \frac{27}{4 \pi^2 N_a^2} \times 7.18 \left(\frac{T}{\theta}\right)^2 \lambda_{i(\infty)} \\ &= \frac{4.93}{\theta^2 N_a^2} T^2 \lambda_{i(\infty)} \end{aligned} \quad (\text{II, 36})$$

where N_a is the number of conduction electrons per atom. Of course, $\lambda_{i(\infty)}$ refers not to the measured electronic thermal conductivity but to the 'ideal' value obtained after taking account of the residual thermal resistivity.

Since the original *Bloch* theory does not take Umklapp processes nor the dispersion of phonons (in other words, the dispersion of the velocity of sound) into account, and these do influence $\lambda_{i(\infty)}$, *Klemens* (1954c) has shown that it would be more appropriate to compare λ_E with the ideal electronic thermal conductivity at low temperatures, λ_i . In this manner, one would be comparing two quantities which are governed by the same mechanisms, thus eliminating the effect of any variation of the interaction constant C with the phonon frequency. Assuming the *Makinson* coupling scheme (that phonons of all polarisations interact equally with the conduction electrons), he obtains for a spherical Fermi surface, at temperatures $T \ll \theta$,

$$\lambda_E = 1/w_E = 313 \lambda_i \left(\frac{T}{\theta_D}\right)^4 N_a^{4/3} \quad (\text{II, 37})$$

This equation is easily obtained by substituting in equation (II, 36), the value of $\lambda_{i(\infty)}$ (given in terms of λ_i , by equation (II, 25)) using *Klemens'* value of 64.0 for the numerical constant. In equation (II, 37) it is appropriate to use θ_D , the Debye temperature obtained from low temperature specific heat measurements, because it is the average over all polarisations.

On the other hand, if one assumes the *Bloch* coupling scheme (namely, that only longitudinal waves can directly interact with the electrons), the equation takes the form

$$\lambda_E = 1/w_E = 105 \lambda_i \left(\frac{T}{\theta_L}\right)^4 N_a^{-4/3} \quad (\text{II, 38})$$

Here we use the value of θ appropriate for longitudinal lattice waves, namely θ_L (*Blackmann*, 1951). Estimation of θ_L in relation to θ_D is not easy for real metals. Monovalent metals like copper and sodium are elastically very anisotropic, so that averaging has to be done over the different directions relative to the crystal axes. Such a calculation has been made by *Blackman* (1951), and usually θ_L is taken to be $\simeq 1.5 \theta_D$. The numerical constant 105 comes in equation (II, 38) in place of 313, because $C_L^2 = C^2/3$. Further, if w_E in the equations (II, 36, 37 and 38) refers to an alloy, λ_i and $\lambda_{i(\infty)}$ also refer to the same alloy, and not to the pure solvent metal.

N_a has sometimes been regarded more or less as an adjustable parameter (see, for instance, *Sondheimer* 1952) and taken to mean the 'effective' number of electrons per atom, defined by the current induced in the band due to an electric field. It seems more reasonable, however, to regard N_a as representing the number of free electrons per atom in the conduction band (see, for instance, *Klemens* 1954c, 1956).

Choice of formula for λ_E :

We have obtained equations (II, 37) and (II, 38) respectively for the *Makinson* and *Bloch* coupling schemes of phonon-electron interactions. If one assumes $N_a = 1$ for pure silver, say, and calculates $\lambda_E (= 1/w_E = T^2/E)$ from these equations, it is found that the *Makinson* scheme gives a value about 15 to 20 times that given by the *Bloch* scheme. It appears therefore that the lattice thermal conductivity λ_E (when only phonon-electron scattering processes exist) depends sensitively upon whether the electrons interact with phonons of all polarisations (*Makinson* scheme) or only with longitudinal phonons (*Bloch* scheme). Direct determina-

tion of λ_E of a pure metal being not possible, the following method is employed for testing which of these schemes holds better.

Considering a series of alloys having one and the same solvent metal, the experimental values of lattice thermal resistivity in the temperature region where it shows a T^{-2} temperature dependence, give E for each of the alloys. We plot E against the solute concentration (*Klemens* 1954a, 1956; *Kemp et al* 1954, 1956). The value (E_0) of E for the pure solvent metal is obtained by extrapolation to zero solute concentration. Since we know the expected values of E_0^{Makinson} and E_0^{Bloch} , for $N_a = 1$, this constitutes an immediate check as to which of these coupling schemes describes the position better. It is quite possible that the value of E_0 lies somewhere between E_0^{Makinson} and E_0^{Bloch} (but closer to the former, say); then we infer that this is an intermediate coupling wherein the transverse phonons do not interact so strongly with conduction electrons as do the longitudinal phonons. Incidentally one can estimate the value of N_a for the pure solvent metal, using the appropriate equation (here, equation (II, 37)).

Coming now to equation (II, 36), we already mentioned that it compares two quantities λ_E and $\lambda_{i(\infty)}$ which pertain to different temperature regions. It would be instructive to use this formula to see how far it deviates from the results obtainable from the formulae (II, 37) and (II, 38), which compare λ_E and λ_i , both of which refer to low temperatures. Combining equations (II, 36) and (II, 34), we obtain

$$1/E = 1/w_E T^2 = \frac{4.93}{\theta^2 N_a^2} \lambda_{i(\infty)} \quad (\text{II, 39})$$

Considering again a series of alloys having one and the same solvent metal, E is obtained for each alloy (as mentioned in the preceding paragraph) from the experimental values of lattice thermal resistivity in the temperature region where it shows a T^{-2} temperature dependence. Since $\lambda_{i(\infty)}$ refers to the 'ideal' thermal conductivity, it appears, at first sight, that equation (II, 39) can be used to calculate the electron concentration N_a in each of the alloys, holding $\lambda_{i(\infty)}$ constant. That would not be correct, because alloying changes, besides N_a , the $\lambda_{i(\infty)}$ (and λ_i) also. $\lambda_{i(\infty)}$ for each alloy is evaluated by measuring the electrical resistivity at the ice-point and the steam-point, and obtaining $d\rho/dT$. Assuming the validity of the *Wiedemann-Franz-Lorenz*

law (which is justified at high temperatures, irrespective of any assumptions regarding band structure and the phonon-electron interaction) and a linear temperature-dependence of ρ_i , at high temperatures, $w_{i(\infty)}$ is calculated thus:

$$\rho_{\infty} = \rho_0 + \rho_{i(\infty)} = \rho_0 + GT$$

where G is a constant of proportionality.

$$\therefore \left(\frac{d\rho}{dT}\right)_{\infty} = G; \quad \text{and} \quad \rho_{i(\infty)} = T \left(\frac{d\rho}{dT}\right)_{\infty}.$$

Now
$$w_{i(\infty)} = \rho_{i(\infty)} / L_e T = \frac{1}{L_e} \left(\frac{d\rho}{dT}\right)_{\infty}$$

$$\therefore \lambda_{i(\infty)} = L_e / \left(\frac{d\rho}{dT}\right)_{\infty} \quad (\text{II, 40})$$

Substituting this value of $\lambda_{i(\infty)}$ in equation (II, 39), N_a for the particular alloy is obtained (Sladek 1955). Plotting N_a against solute concentration and extrapolating to zero solute concentration, N_a for the pure solvent metal can be estimated. We wish to emphasize here that, for reasons given in connection with equation (II, 36), we cannot attach much weight to the value obtained for N_a from that equation. Our only interest is to see how far this value of N_a deviates from that obtained as indicated in the previous paragraph, employing equation (II, 37).

Chapter III

The Silver-base alloys

§ 1. Introduction

Norbury (1921) enunciated the rule known after him: "the increase in resistance caused by a certain impurity (expressed in atoms per cent) increases both with the distance in the series of the periodic system and the distance in the columns, in which the metal and admixture lie". Stated otherwise, this rule requires that for alloys consisting of elements of different valencies, the atomic (electrical) resistivity increase should be proportional to the square of the valency difference between the solvent and solute metals. The measurements by *Borelius* at room temperature and at solid carbon-di-oxide temperature, on binary alloys containing a small amount of transitional metal as solute, showed that the behaviour of these alloys was not in conformity with *Norbury's* rule. The interesting series of investigations by *Gerritsen* and *Linde* (1951 a, b, 1952, 1953) on these alloys at lower temperatures resulted in revealing their anomalous residual electrical resistance and negative (electrical) magneto-resistance effects. To explain these results, *Korringa* and *Gerritsen* (1951, 1953) postulated a new theory incorporating a "hitherto unknown feature of the interaction between the conduction electrons" which shows out in the presence of an impurity.

The present measurements on Ag-Mn alloys (containing 0.55, 0.32 and 0.14 atoms per cent of Manganese) constitute essentially an extension of the above-mentioned investigations to the aspect of thermal conductivity. A preliminary report on the behaviour of Ag-0.55%Mn has already been presented (*De Nobel* and *Chari*, 1955) at the International Conference on Low temperature Physics, Paris, 1955. An alloy of Ag-In (containing 0.24 atoms per cent of Indium) was also included in this series so as to distinguish between the behaviour of the noble metal alloys containing a magnetic and a non-magnetic solute.

§ 2. Preparation of the alloys and determination of the solute concentration

The alloys *) were prepared a few years back by *Dr. J.O.Linde* from pure silver (analysis not available) and from high purity Manganese and Indium, containing less than 5×10^{-5} parts of impurity. The metals were melted in evacuated silica tubes in a high-frequency furnace, rolled and cut into rods of cross-section about 2.5 mm square.

The electrical resistance of these rods was determined as described in chapter I, § 6, by keeping them directly immersed in the bath liquids. Further, their resistances at the temperature of melting ice and at steam temperature were also measured. The determination of solute concentration in the alloys was as follows (*Linde* 1939, *Gerritsen* and *Linde* 1951a):

Representing the electrical resistivities of the alloy and of pure silver, at a given temperature, by ρ^{alloy} and ρ^{Ag} , we can denote the resistivity increase on alloying, by $\Delta\rho$, where

$$\Delta\rho = \rho^{\text{alloy}} - \rho^{\text{Ag}} \quad (\text{III}, 1)$$

If c is the concentration of solute metal expressed in atoms per cent, and $\delta\rho$ the atomic resistivity increase (that is, the resistivity increase due to one atom per cent of solute metal), it is well-known that for small values of c , one could consider $\Delta\rho$ as being equal to $c\delta\rho$. This relation was experimentally verified by *Linde* at room and at other temperatures, for Silver-Manganese and Silver-Indium alloys, among others. *Linde* (1939, 1948) also showed that the value of $\delta\rho$ for Ag-Mn alloys (containing small amounts of Manganese) was $1.60 \mu\Omega\text{-cm}$. From his other data, we derived also

$$\rho_{273^{\circ}\text{K}}^{\text{Ag}} = 1.465 \mu\Omega\text{-cm}; \quad \rho_{373^{\circ}\text{K}}^{\text{Ag}} = 2.084 \mu\Omega\text{-cm};$$

and $\delta\rho$ for Ag-In alloys containing small amounts of Indium = $1.765 \mu\Omega\text{-cm}$. Connecting the electrical resistance R and the electrical resistivity ρ by a proportionality factor 'a', we can write

*) We thank *Dr. J.O.Linde* (of the Institute for Physics, Royal Technical High School, Stockholm, Sweden) and *Dr. A.N.Gerritsen* (formerly of the Kamerlingh Onnes Laboratory, Leiden; now Associate Professor of Physics at the University of Lafayette, Indiana, U.S.A.) for making these rods available to us for the investigations described in this thesis.

$$R_{273^{\circ}\text{K}}^{\text{alloy}} = a \cdot \rho_{273^{\circ}\text{K}}^{\text{alloy}} = a (\rho_{273^{\circ}\text{K}}^{\text{Ag}} + c \cdot \delta\rho)$$

$$R_{373^{\circ}\text{K}}^{\text{alloy}} = a \cdot \rho_{373^{\circ}\text{K}}^{\text{alloy}} = a (\rho_{373^{\circ}\text{K}}^{\text{Ag}} + c \cdot \delta\rho)$$

Eliminating 'a', we obtain,

$$c = \frac{R_{273^{\circ}\text{K}}^{\text{alloy}} \cdot \rho_{373^{\circ}\text{K}}^{\text{Ag}} - R_{373^{\circ}\text{K}}^{\text{alloy}} \cdot \rho_{273^{\circ}\text{K}}^{\text{Ag}}}{\delta\rho (R_{373^{\circ}\text{K}}^{\text{alloy}} - R_{273^{\circ}\text{K}}^{\text{alloy}})} \quad (\text{III, 3})$$

Of course, in determining the Manganese or Indium content in the alloy, the corresponding value of $\delta\rho$ has to be used.

Following this procedure, we obtained for the three Ag-Mn rods, Manganese concentrations of 0.55, 0.32 and 0.14 respectively, while in the Ag-In rod, the Indium concentration was found to be 0.24 atoms per cent.

§ 3. The residual electrical resistivity, ρ_0

Fig. III,1 gives the variation of the electrical resistivities of the four rods with temperature. It can be seen that they all attain a nearly constant value at liquid Hydrogen temperatures; but whereas the the Ag-0.24%In rod maintains this value even at the liquid Helium temperatures, the other rods show an anomalous fall of resistance in the liquid Helium region itself. Further, in the case of the Ag-0.55%Mn rod, the value obtained for ρ_0 , the residual electrical resistivity, by extrapolating the electrical resistivity versus temperature curve, to the absolute zero of temperature, led to the difficult situation of the measured thermal conductivity being somewhat less than the estimated electronic thermal conductivity $\lambda_e (= L_0 T / \rho_0)$, where L_0 is the ordinary Lorenz parameter: see equation II, 30). We adopted the only course left, namely, to consider the constant value attained at liquid Hydrogen temperatures, as the residual resistivity ρ_0 , looking upon the further fall of ρ as an anomaly. For the sake of uniformity, the same convention was applied to the rest of the rods as well.

In fig. III,2 where λ/T is plotted against T , the horizontal lines through the points marked L_0/ρ_0 on the Y-axis, give the estimated value of λ_e/T . In order to obtain the lattice thermal conductivity λ_g at any temperature, one has to measure the length of the corresponding ordinate intercepted between the λ/T versus T curve and the horizontal line (drawn through the point marked

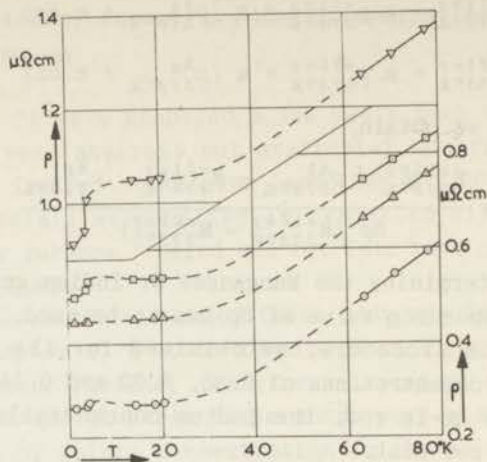


Figure III, 1
 Silver-base alloys: Electrical resistivity ρ
 in $\mu\Omega\text{cm}$, versus Temperature.
 ∇ Ag-0.55%Mn. \triangle Ag-0.24%In.
 \square Ag-0.32%Mn. \circ Ag-0.14%Mn.

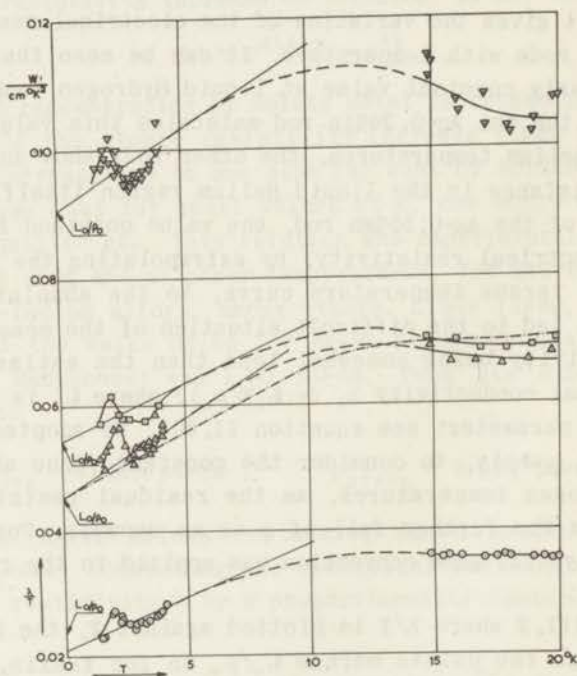


Figure III, 2
 Silver-base alloys: λ/T in watts/cm-deg²,
 versus Temperature.
 \circ Ag-0.55%Mn. \square Ag-0.24%In.
 \triangle Ag-0.32%Mn. ∇ Ag-0.14%Mn.
 The curve marked -.- is for Cu-0.056%Fe
 (White and Woods).

L_o/ρ_o). This portion of the ordinate gives λ_g/T . Since theory requires λ_g to vanish at 0°K, it is seen by extrapolation of the λ/T vs T curve to 0°K, that our choice of ρ_o was proper. It will be seen from the figure that in the case of Ag-0.55%Mn, the extrapolated curve meets the λ/T axis at a point about 10% lower than the experimental value of L_o/ρ_o . This difference is not serious. For this rod, we have throughout used this value obtained by extrapolation, as the proper one.

§ 4. Electronic thermal resistivity, w_e

We have seen in chapter II that

$$w_e = w_i + w_o \quad (\text{II}, 20)$$

Rather than use the theoretical expression for w_i given by equation (II, 24), we have preferred the experimental value of *White* (1953b) for annealed pure silver, namely,

$$w_i = 1.06 \times 10^{-5} T^{2.5} \text{ cm-deg/watt} \quad (\text{III}, 4)$$

Of course, $w_o = \beta/T = \rho_o/L_o T$, ρ_o being the residual electrical resistivity. From our experimental values of ρ_o , it was found that for the Ag+0.55%Mn, the w_i term amounted to < 1% of w_o at 20°K becoming negligible at lower temperatures. For the alloy of smallest manganese content, namely Ag-0.14%Mn, w_i was about 4% of w_o at 20°K, and 1.5% at 15°K, falling rapidly to insignificance at lower temperatures. In fig. III, 3, of λ vs T , of these alloys, the curves marked λ_e are thus the function

$$\lambda_e = 1/w_e = \left(\frac{\rho_o}{L_o T} + 1.06 \times 10^{-5} T^{2.5} \right)^{-1} \quad (\text{III}, 5)$$

The values used for ρ_o for the four alloys in order of decreasing solute content are 1.17, 0.54, 0.45 and 0.27 $\mu\Omega\text{cm}$.

Table III, 1 gives λ of the four silver-base alloys as a function of T .

§ 5. Discussion

The λ versus T curves (fig. III.3):

The change in shape at about 30°K in the curves for these alloys is, of course, due to the lattice thermal conductivity

Table III, 1
Silver-base alloys: λ (in watts/cm-deg) against T°K.

Ag-0.55%Mn		Ag-0.32%Mn		Ag-0.24%In		Ag-0.14%Mn	
T	λ	T	λ	T	λ	T	λ
3.806	0.101 ²	4.081	0.234	3.930	0.236	4.045	0.422
3.077	0.078 ³	3.512	0.190	3.392	0.196	3.760	0.367
2.273	0.058 ⁴	3.194	0.171	2.800	0.162	3.466	0.335
1.963	0.052 ⁸	2.906	0.148	2.446	0.142	3.185	0.303
1.471	0.034 ⁰	2.723	0.141	2.328	0.137	2.944	0.277
		2.572	0.138	2.000	0.123	2.747	0.263
3.916	0.106 ⁴	2.330	0.132	1.585	0.091	2.536	0.246
3.426	0.088 ⁰	2.119	0.119			2.337	0.225
2.858	0.069 ⁷	1.925	0.104	19.73 ⁴	1.385	2.108	0.215
2.277	0.059 ⁷	1.782	0.094 ³	18.32 ⁸	1.237	1.916	0.189
1.554	0.035 ⁹	1.512	0.075 ⁵				
				19.88 ⁴	1.395	4.028	0.402
4.122	0.116 ⁸	4.077	0.225	17.89 ⁷	1.228	3.737	0.363
3.742	0.099 ⁰	2.852	0.149	16.87 ⁴	1.158	3.443	0.329
3.262	0.082 ⁷	1.562	0.080 ⁵	15.88 ⁵	1.114	3.155	0.304
2.906	0.073 ⁴			14.69 ⁰	1.035	2.948	0.278
2.605	0.065 ⁷	4.048	0.228			2.727	0.258
2.308	0.059 ⁸	3.796	0.208	75.47	2.236	2.439	0.244
1.983	0.054 ¹	3.695	0.197	72.72	2.304	2.141	0.210
		3.596	0.189	67.27	2.232	1.835	0.178
19.95 ⁹	0.704	3.549	0.187	64.46	2.242		
19.37 ⁸	0.689	3.497	0.186			2.886	0.277
18.96 ⁰	0.668	3.395	0.183			2.419	0.238
18.02 ⁷	0.643	3.312	0.179			1.899	0.190
17.47 ⁶	0.620	3.034	0.162			1.563	0.152
16.97 ⁸	0.599						
16.04 ⁹	0.573	19.70 ⁴	1.343			19.85 ⁹	2.082
15.30 ⁶	0.544	18.77 ⁴	1.251			18.89 ⁶	1.922
14.82 ³	0.532	17.73 ⁸	1.173			17.95 ⁹	1.842
		16.67 ⁴	1.112			17.07 ⁰	1.847
75.48	1.348	15.70 ⁰	1.046			15.96 ⁷	1.704
70.98	1.285	14.84 ³	1.025				
67.46	1.260					19.97 ⁴	2.148
		76.24	2.333			19.77 ¹	2.121
86.51	1.406	73.34	2.274			19.02 ⁶	1.981
81.58	1.361	70.86	2.262			18.08 ²	1.845
77.39	1.328	67.96	2.227			17.10 ³	1.765
73.98	1.286	65.35	2.192			16.04 ⁰	1.688
		65.33	2.190			14.86 ⁵	1.648
						73.84	2.618
						70.32	2.616

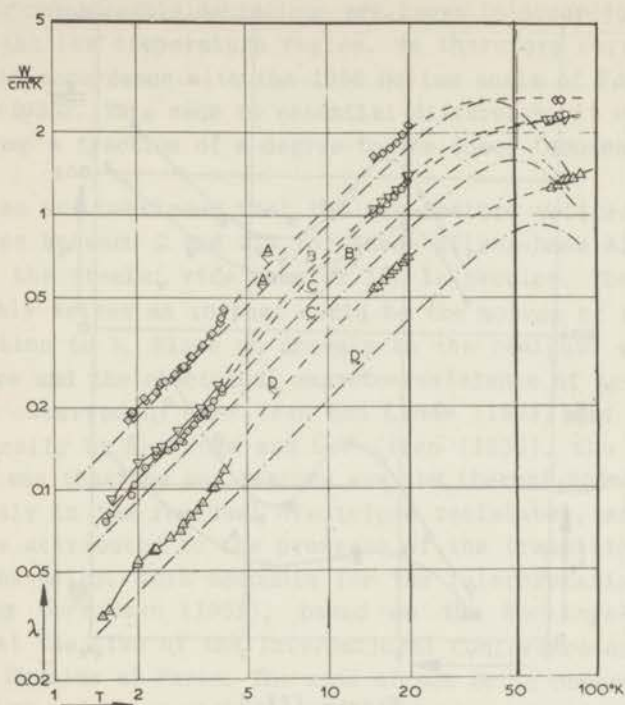


Figure III, 3
 Silver-base alloys: λ and λ_e both in watts/cm-deg.
 versus Temperature.
 Δ Ag-0.55%Mn (curve D); ∇ Ag-0.24%In (curve B).
 \circ Ag-0.32%Mn (curve C); \diamond Ag-0.14%Mn (curve A).
 The curves marked A', B', C' and D' (and drawn -.-.-)
 are the λ_e curves corresponding respectively to the λ
 curves marked A, B, C and D.

attaining its maximum value near about this temperature. The main point of interest, however, is in the liquid Helium region where, with fall of temperature, λ ceases to fall but remains nearly constant over a small temperature region. Taking, for instance, the case of Ag-0.32%Mn, this region lies between about 2.7 and 2.4°K. (The λ/T versus T curves show this as a hump and the λ_g versus T curves of fig. III, 4, also show it in a marked way). The effect of this small region of nearly temperature-independent λ is to shift the curve more or less parallel to itself, to a higher λ -value than would otherwise result if the λ versus T curve were simply extended to the lower temperatures. Measurements at low temperatures on dilute copper alloys by White and Woods (1954,

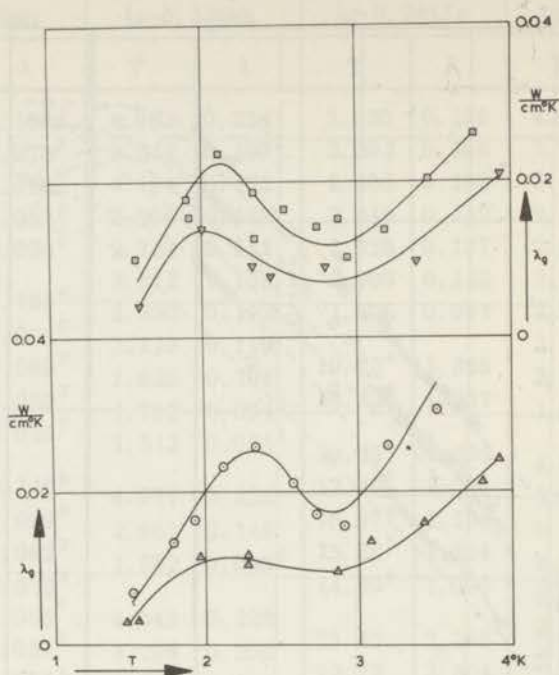


Figure III, 4
 Silver-base alloys: λ_g in watts/cm-deg,
 versus Temperature.
 Δ Ag-0.55%Mn. ∇ Ag-0.24%In.
 \circ Ag-0.32%Mn. \square Ag-0.14%Mn.

1955), on silver alloys by Kemp et al (1954, 1956) and on Indium-Thallium alloys by Sladek (1955) do not show this feature. We had therefore to test its genuineness.

For the Ag-0.55%Mn rod, which was the first of this series of alloys to be investigated by us, our original measurements employed Allen-Bradley carbon composition resistors. The measurements were repeated using phosphor-bronze thermometers and since the agreement was excellent, we made bold to make a preliminary announcement of our results at the International Conference on Low Temperature Physics, Paris (*De Nobel and Chari*, 1955). Later, we repeated the measurements using the *De Vroomen* carbon-film resistors and there was perfect agreement, as can be seen from the three sets of points marked on the λ versus T curve for Ag-0.55%Mn, at liquid Helium temperatures - (vide fig. III, 3 and III, 5).

Originally, we had used the 1948 Helium vapour pressure scale, for which considerable deviations are known to occur just at this part of the low temperature region. We therefore corrected our results in accordance with the 1956 Helium scale of *Van Dijk* and *Durieux* (1955). This made no essential difference; it only shifted the hump a fraction of a degree to the lower temperature side.

Thus we are convinced that the new feature noticed by us in the region between 2 and 3°K for these silver-base alloys (and also for the steels; vide chapter IV) is genuine. The question immediately arises as to what could be the source of this extra contribution to λ . Since an anomaly in the residual electrical resistance and the electrical magneto-resistance of Ag-Mn alloys had been observed by *Gerritsen* and *Linde* (1951) and discussed theoretically by *Korringa* and *Gerritsen* (1953), the first impression was that the new feature was the thermal counterpart of the anomaly in the residual electrical resistance, and that it should be attributed to the presence of the transitional metal ion in the alloy. This accounts for the interpretation of this effect by *Gerritsen* (1955), based on the *Korringa-Gerritsen* theory, at the time of the International Conference on Low Temperature Physics at Paris. The same effect being observed in the Ag-In alloy and later with the steels, however, entirely altered the picture.

Our preliminary communication to the International Conference on Low Temperature Physics, Paris, 1955, contained a fallacy, in that the fig. 1, therein, depicted a flattening of the hump of the λ/T versus T curve on the application of increasingly strong magnetic fields. That was based on insufficient data. We have now made a few series of measurements in magnetic fields and fig. III,5 represents the results. It can be seen that the shape of the λ versus T curve persists, without any significant change, even in the strongest fields used, and should therefore be a feature of the lattice thermal conductivity. Further, since it is found in solids of such a different nature as dilute silver alloys and complex alloys like the steels (where we have a primary substitutional solid solution of Fe and Ni or Mn, forming an interstitial solid solution of carbon), it is evidently of a rather general nature.

Measurements on dielectric solids by *De Haas* and *Biermasz* (1935, 1937) and *Berman* (1953), among others, do not show this effect, whereas the measurements on quartz glass by *Wilkinson* and

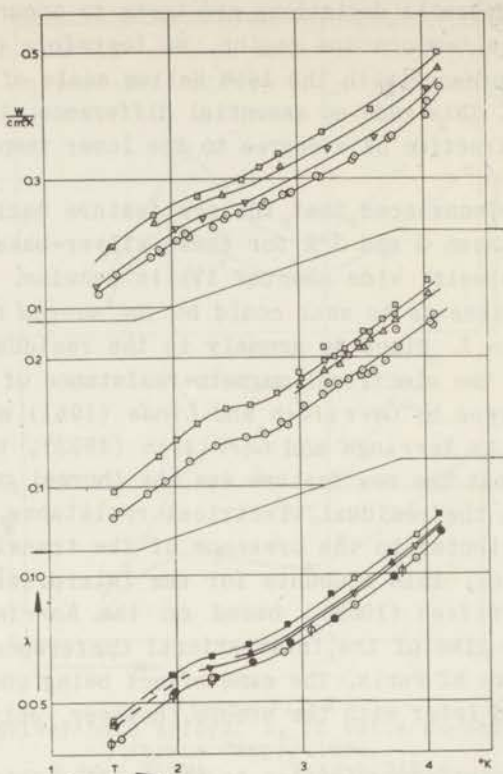


Figure III, 5
Silver-base alloys: λ in watts/cm-deg,
versus Temperature.

○, ◊, ●: $H = 0$; ◒: $H = 12 \text{ K}\Phi$;
△, ▲: $H = 19 \text{ K}\Phi$; ■, □: $H = 25.5 \text{ K}\Phi$.
The set of four curves at the top are
for Ag-0.14%Mn. The set of three curves
at the middle are for Ag-0.32%Mn. The
set of four curves at the bottom are
for Ag-0.55%Mn. Data for Ag-0.24%In are
not plotted since the effect of magnetic
field us not measurable.

Wilks (1949) and by Berman (1951a) show something akin to this, in having a narrow region of temperature-independent λ . In pure metals, lattice thermal conduction is masked by the electronic thermal conduction, and plays such an insignificant role that we do not expect this feature in lattice thermal conduction to be noticeable. In very impure metals and in alloys containing a fairly large amount of solute metal, impurity scattering of the phonons begins to take effect at temperatures probably as low as

liquid Helium temperatures, so that the effect would not be quite marked. This leaves 'suitably' dilute alloys to be the material wherein one should look for this effect. Further discussion of this topic will be taken up under "the interaction between phonons and electrons".

The λ/T versus T curves:

In fig. III, 2 is plotted λ/T versus T for the silver-base alloys measured by us. For purposes of comparison, a few of the measured points of *White* and *Woods* (1955) on Cu-0.056%Fe (as read off the graph in fig. 5, of their paper), are also plotted. It was evident to us at the very outset, that the anomaly in the thermal conductivity at the liquid Helium temperatures would make it rather a difficult matter for the analysis of our measurements. The theoretical prediction of *Makinson* (1938) and the experimental results - of *Hulm* (1951) and *Estermann* and *Zimmermann* (1952) on Copper-Nickel alloys, of *Berman* (1951b) on industrial alloys, of *White* and *Woods* (1954, 1955) on very dilute Copper-Iron alloys, of *Sladek* (1955) on Indium-Thallium alloys, and of *Kemp* et al (1954, 1956) on Silver-Palladium and Silver-Cadmium alloys - have shown that at sufficiently low temperatures, lattice thermal conduction is limited mainly by the phonons being scattered by the conduction electrons (the E/T^2 term in the equations II, 32 and II, 34). We have, therefore, as a first approximation, ignored the anomaly in the liquid Helium region. In other words, we considered it rather as a spread of points, and boldly drew a straight line through the point marked L/ρ_0 ($= 1/w_0 T$) on the Y-axis. The correspondence with *White* and *Woods'* curve for Cu-0.056%Fe, lends support to this step. The gradient of this line equals $1/E$, whence the phonon-electron scattering coefficient E for each of the alloys is obtained. Boundary scattering of the phonons is also probably present but we neglected it, considering that *Berman* (1951b) has shown this to be at most about 1/2% of the total thermal resistivity, for a grain size of the order of 0.02 mm; and our alloy specimens have certainly much larger grain sizes.

The values of E thus obtained for the Silver-base alloys are respectively 570, 400, 540 and 400 $\text{cm-deg}^3/\text{watt}$, in the order of decreasing solute concentration. Remembering that this estimate includes dislocation scattering of the phonons, and that we do not expect the addition of such small percentages of solute atoms to significantly affect E , we take 400 as a reasonable value for

E of pure Silver. The comparatively higher value of E in the case of Ag-0.55%Mn and Ag-0.24%In should be attributed to dislocations. The value of E = 400 is in keeping with the estimate of E = 430 for pure Silver (assuming $N_a = 1$) on the *Makinson* scheme (see *Kemp et al* 1956), whereas it should be 8300 on the *Bloch* coupling scheme. Thus our measurements show that in the case of Silver, the conduction electrons interact more or less equally strongly with longitudinal and transverse phonons. From a discussion of the various conduction properties of monovalent metals, *Klemens* (1954c) was led to expect this behaviour, and this has already been confirmed for Silver by *Kemp et al* (1954, 1956), and for Copper by *Klemens* (1954a) and by *White and Woods* (1954, 1955).

Using the value $\alpha = 5 \times 10^{-5}$ (*Rosenberg* 1954a) and of E = 400 we can estimate N_a for pure silver thus:

$$\lambda_g = T^2/400 ; \quad \lambda_i = 1/\alpha T^2 ;$$

and $\theta = 215^\circ\text{K}$. But, from equation (II,37),

$$\lambda_g/\lambda_i = 313 (T/\theta)^4 \cdot N_a^{-4/3}$$

Therefore, $N_a \simeq 1.1$.

Going back to the λ/T versus T curves, we find that they deviate from rectilinearity (as does also the curve of *White and Woods*) above about 6-7°K. The lowering of the curves below the straight lines indicates the setting-in of phonon-impurity scattering, and this is in agreement with the requirements of *Makinson's* theory. It appears, *a priori*, from the relative depressions of the curves below rectilinearity, that the first small additions of impurity (or solute atoms) are much more effective in scattering phonons than are further additions. It would however need more detailed study over a whole series of impurity concentrations, before definite conclusions can be drawn.

Though we do not have measurements at temperatures intermediate to liquid Hydrogen and liquid Helium temperatures, the trend of the λ/T versus T curve in these two regions, points to the existence of a maximum in the intermediate temperature region. This could be explained. For, at these intermediate temperatures, where mutual scattering of phonons can be neglected, we have

$$\lambda_g = 1/w_g = \frac{1}{\frac{B}{T^3} + \frac{E}{T^2} + DT}$$

(from equations II,9, 11, 34, 35), so that

$$\lambda_g/T = \frac{1}{\frac{B}{T^2} + \frac{E}{T} + DT^2} \quad (\text{III}, 6)$$

For λ_g/T to be maximum, we should have the minimum value for $(B/T^2 + E/T + DT^2)$, which would be the case if $2DT^4 = ET + 2B$. As mentioned above, the boundary scattering term is likely to amount to only a few per cent, so that we can write the condition as

$$2 DT_{\max}^3 = E \quad (\text{III}, 7)$$

To test this conclusion, we took up the measured points at liquid Hydrogen temperatures and tried to split the lattice thermal resistivity into that due to scattering by electrons and due to scattering by impurities and defects. Then

$$w_g = \frac{E}{T^2} + DT \quad \text{or} \quad w_g T^2 = E + DT^3 \quad (\text{III}, 8)$$

Plotting $w_g T^2$ against T^3 should give a straight line from which E and D could be found out. Actually, the plotted points are rather scattered: the spread being $\pm 5\%$ for Ag-0.55%Mn and Ag-0.32%Mn and as much as 20% and 35% respectively for Ag-0.24%In and Ag-0.14%Mn.

Since we cannot expect two resistance mechanisms with such diversity in temperature-dependence (especially when they are of comparable magnitudes) to be strictly additive, and since we only wished to have a rough idea of the relative magnitudes of the two resistance components, we made estimates of the values of E and D from the straight lines drawn symmetrically through the rather scattered points. Table III,2, gives the values of E and D obtained in this manner, compared with the value of E obtained from the Helium temperature data.

The values for E in the last column are obtained thus: In double logarithmic plots of w_g versus T , there are short temperature regions just above the liquid Helium temperatures, where the extrapolated curves indicate a proportionality of w_g with T^{-2} , suggesting that phonon-electron scattering is dominant in these short intervals. From the values of λ at these temperatures, a rough estimate of E could be made.

Using the values of E and D , we have employed equation III,7, for estimating the temperature (T_{\max}) at which λ_g/T would attain its maximum value, and also the corresponding (maximum) value of λ_g/T . Table III,3 gives the values thus obtained for T_{\max} and

Table III, 2

Specimen	D in cm/watt	E in cm-deg ³ /watt		
		From $w_g T^2$ vs T^3 curves at liquid Hydrogen temperatures	From λ/T vs T curves at liquid Helium temperatures	From w_g vs T curves covering liquid Hydrogen and Helium temperatures
Ag-0.55%Mn	0.082	750	570	720
Ag-0.32%Mn	0.066	460	400	400
Ag-0.24%In	0.092	560	540	425
Ag-0.14%Mn	0.147	400	400	510

Table III, 3

Specimen	T_{max}		$(\lambda_g/T)_{max}$ in W/cm-deg ²	
	calc.	obs.	calc.	obs.
Ag-0.55%Mn	16.5°K	13.0°K	0.015	0.015
Ag-0.32%Mn	15.5°K	12.5°K	0.022	0.024
Ag-0.24%In	14.5°K	12.5°K	0.017	0.017 ⁶
Ag-0.14%Mn	11.1°K	11.5°K	0.018	0.022

$(\lambda_g/T)_{max}$, against their experimental values. We consider the agreement good. We find, on the whole, such a method of estimating the approximate values of T_{max} and $(\lambda_g/T)_{max}$ to be very instructive.

Interaction between phonons and electrons, and coupling between longitudinal and transverse phonons:

For the discussion of the interaction between conduction electrons and the phonons, three possibilities arise.

Case 1: The electrons interact equally strongly with the longitudinal as well as with the transverse phonons: (Makinson coupling scheme), so that $C_L^2 = C_T^2$.

Case 2: The electrons interact directly with the longitudinal phonons but less strongly (or even not at all) with the transverse phonons, the latter being closely coupled to the longi-

tudinal phonons, by means of ordinary (non-umklapp) three-phonon processes. Thus $C_L^2 \gg C_T^2$ and C_T^2 might even be zero.

We wish to make the following comments as regards case 2: i) The assumption of a spherical Fermi surface and of spherical symmetry of the crystal lattice potential lead to $C_T = 0$, whilst $C_L \approx \zeta$. ii) Since the transverse phonons do not strongly interact with the conduction electrons, one might jump to the conclusion that the lattice thermal conductivity would be nearly as large as in an equivalent dielectric solid. The close coupling between the longitudinal and transverse phonons, however, tends to equalise the effective mean free paths of phonons having the same frequency but different polarisation: and this effective mean free path would be governed by the scattering of the longitudinal phonons.

Now, let us go back to equation (II, 33). The lattice thermal conductivity λ_E is there expressed in terms of C_L^2 , and is independent of θ . Thus cases 1 and 2 would both lead to the same value of λ_E , provided it is expressed in terms of C_L^2 .

Case 3: The transverse phonons interact less strongly, if at all, with the conduction electrons and are, further, only loosely coupled to the longitudinal phonons. The transverse phonons could therefore contribute to lattice conduction without being considerably influenced by electron interactions. This would result in an additional contribution to the lattice thermal conductivity (Klemens 1954a, 1956). We think this might be the cause for the anomaly in thermal conductivity in the liquid Helium region, observed by us.

The reasons why we have been able to detect this feature are i) carbon resistance thermometry at the liquid Helium temperatures becomes more sensitive and dependable than the gas thermometry employed by most other investigators; ii) this effect seems more marked in 'suitably' dilute alloys. We say 'suitably' dilute, since neither the very dilute copper alloys of *White and Woods*, nor the very high solute-content alloys (like the Ag-Pd and Ag-Cd alloys of *Kemp et al*, the In-Tl alloys of *Sladek*, the Cu-Ni alloys of *Hulm* and of *Estermann and Zimmermann*, and the industrial alloys studied by *Berman*) show it. In fact, in the higher Nickel-content steels measured by us (nos. 1287I, 1798H and 3754) the effect is quite small. It will be shown in the next chapter that the measurements of some of the other investigators also show indications of this effect in their specimens, though not to a marked extent.

Analogy can be drawn between this additional transverse phonon

contribution to the lattice thermal conductivity and the so-called 'longitudinal' conductivity in quartz glass (see *Berman* 1951a, *Klemens* 1954a, 1956).

The applicability of the *Korringa-Gerritsen* model to the present case:

Since the *Korringa-Gerritsen* model could account for the anomalous features in the residual electrical resistance and electrical magneto-resistance of dilute Ag-Mn alloys (and other alloys of a transitional metal in a noble metal), one wonders to what extent it can explain the anomalous behaviour of the thermal conductivity. The increase in thermal conductivity of these alloys on application of strong magnetic fields at liquid Helium temperatures can be qualitatively explained by the *Korringa-Gerritsen* model as being due to the fact that the anomalous scattering for electrons with spins anti-parallel to the oriented magnetic ions (see *Gerritsen*, 1955) is cut off. We have not yet made a detailed analysis of the thermal conductivity measurements in magnetic fields, so as to test whether the model could quantitatively account for the variation of the thermal magneto-resistance with temperature, field strength and manganese content.

We have suggested in chapter III that the anomaly in the thermal conductivity seems to be a feature of the lattice conductivity. It would not therefore, come within the scope of the *Korringa-Gerritsen* model.

Chapter IV

The Steels

§ 1. Introduction

Steels are iron-carbon alloys, their characteristic properties depending on the fact that carbon forms an interstitial solid solution in γ -iron (austenite) but not appreciably in α -iron. Other metallic or non-metallic elements are also present, whether occurring as impurities or introduced on purpose, during the smelting process. The terms 'plain carbon steels' and 'straight carbon steels' are employed when this additional element content is small, and the material can be considered a pure iron-carbon alloy. 'Special steels' or 'alloy steels' are those wherein a finite amount of a specific element has been added deliberately so as to give certain desired properties to the resulting steel. Thus we have Cobalt steels, Nickel steels, Vanadium steels and so on. In general, the carbon content in steels is small, mostly lying in the range 0.15 to 1.5 per cent by weight. Heating the plain carbon steels to a high temperature for a sufficiently long time makes them single-phase austenitic (face-centred cubic) alloys. Such an 'austenisation' followed by air-cooling gives a 'normalised' steel. In order to ensure a more uniform structure, the cooling process is sometimes slowed down by letting the material cool in the furnace itself. Such a steel is referred to as an 'annealed' steel. The four Nickel steels (nos. 1287D, 3703, 1287I and 1798H) investigated by us, come under this category. The stainless steel (no. 3754) was water-quenched after being heated to the austenitic region.

Studies on the mechanical properties of steels at low temperatures were pioneered by *Hadfield* (1904, 1921, 1933), in collaboration with *Dewar*, *Kamerlingh Onnes* and *De Haas*. A large number of steels was also placed by *Hadfield* at the disposal of the *Kamerlingh Onnes* Laboratory, Leiden. Low temperature thermal conductivity measurements (down to liquid Hydrogen temperatures) on a good number of these have been made by *De Nobel* (1951) using gas and lead resistance thermometry. The present investigation is an extension of *De Nobel's* extensive measurements on steels, to

liquid Helium temperatures. Such studies on steels and other low-conductivity alloys supply information which would be of use in the design of cryogenic equipment (vide *Wilkinson and Wilks* 1949, *Wexler* 1951, *Berman* 1951b). They also furnish data for testing theoretical predictions on the temperature variation of the electronic and lattice components of thermal conductivity in diverse types of solids.

Earlier studies in this direction were made by *Jaeger and Diesselhorst* (1900) on Carbon and Silicon steels, and by *Grüneisen* (1900) and *Lees* (1908) on Carbon steels. There has been more recent work on Carbon steels by *De Nobel* (1951) and by *Powers, Ziegler and Johnston* (1951). Corrosion-resisting steels were investigated by *Karweil and Schäfer* (1939), *Zlunitzin and Saveljev* (1939), *Saveljev* (1941), *Wilkinson and Wilks* (1949), *Schmeissner and Meissner* (1950), *Berman* (1951b), *De Nobel* (1951), *Powers, Ziegler and Johnston* (1951), *Estermann and Zimmermann* (1952) and *Tyler and Wilson* (quoted in N.B.S. Circular, No. 556). Preliminary measurement on a stainless steel (No. 3754) was reported by *De Nobel and Chari* (1955).

Table IV, 1 gives the compositional and other details of the various steel rods discussed in this chapter.

Table IV, 1

The steels: Compositional and other details.

Steel type	Diameter of rod	Heat treatment	Brinell hardness	Percentual composition						
				C	Si	Mn	Cr	Ni	P	S
1287D	5½ mm	Heated to 800°C and cooled in furnace.	153	0.14	0.21	0.72		1.92		
3703	7½ mm	Ibidem.	157	0.11	0.16	0.34		5.10	0.041	0.04
1287I	5½ mm	Ibidem.	277	0.18	0.22	0.93		11.39		
1798H	7½ mm	Ibidem.	179	0.43		1.09		19.64		
3754	7½ mm	Heated to 1150° and quenched in water.	172	0.12	0.43	0.24	18.80	8.10		

§ 2. The electrical and thermal resistivities

The residual electrical resistivity, ρ_0 :

The electrical resistivity curves for the steels are given in fig. IV,1. It is seen that the resistivities of the steels no. 1287D, 3703, and 3754 are constant in the liquid Hydrogen region and stay constant to within 1%, in the liquid Helium region as well. In these cases, there is no difficulty in choosing a value

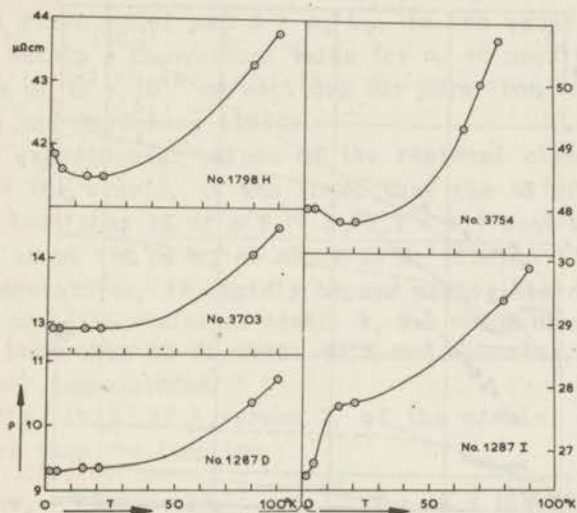


Figure IV,1
The steels: Electrical resistivity ρ
in $\mu\Omega\text{cm}$, versus Temperature.

for ρ_0 , the residual electrical resistivity. For the 1798H steel, there is a slight rise in resistivity at the lowest temperatures. We have taken for ρ_0 , the value of ρ at the minimum of the ρ versus T curve. In any case the difference amounts to $\approx 1\%$ and is not serious. For the 1287I steel, there is a considerable fall in resistivity with temperature, at the lowest temperatures, having stayed approximately constant in the liquid Hydrogen region. There was a similar situation in the case of the silver-base alloys (see chapter III, § 3) and we had to use for ρ_0 , the constant value attained at liquid Hydrogen temperatures, looking upon the further fall of ρ as an anomaly. The alternative procedure of using for ρ_0 , the value extrapolated to 0°K , led to the difficult situation of the measured thermal conductivity in the

case of the Ag-0.55%Mn rod, being considerably less than the estimated electronic thermal conductivity $\lambda_e (= L_o T / \rho_o)$. We thus chose as a uniform policy, the constant value attained at liquid Hydrogen temperatures, as the appropriate value for ρ_o .

In fig. IV, 2, where λ/T is plotted against T , the horizontal lines through the points marked L_o/ρ_o on the Y-axis give the estimated value of $\lambda_e/T (= L_o/\rho_o)$. It can be seen by extrapolation of the curves to 0°K, that our choice of ρ_o is proper.

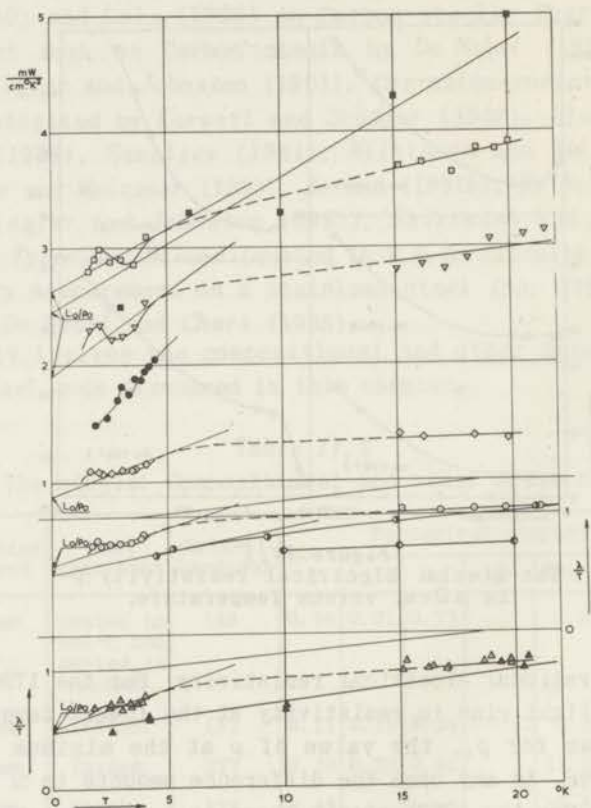


Figure IV, 2
The steels: λ/T in mw/cm-deg^2 , versus Temperature.
 \square 1287D, ∇ 3703, \diamond 1287I, \circ 1798H, \triangle 3754, \blacksquare Karweil and Schäfer, \bullet Wilkinson and Wilks, \circ Berman, \blacktriangle Estermann and Zimmermann, \bullet Hulm (Cu₈₀Ni₂₀).

The thermal resistivity:

We have seen in chapter II that for temperatures below about $\theta/10$, Makinson's theoretical expression for electronic thermal

resistivity can be written, to a good approximation, in the form

$$w_e = w_i + w_o = \alpha T^2 + \beta/T \quad (\text{II, 26})$$

where the first term on the right hand side is the 'ideal' thermal resistivity (caused by the scattering of the electrons by the thermal vibrations of the ionic lattice) and the second is the 'impurity' or 'residual' thermal resistivity (caused by the scattering of the conduction electrons by the impurity atoms and small-scale lattice defects). α is known to be reasonably constant for a given metal and $\beta = \rho_o/L_o$, in the usual notation. Rather than obtain a theoretical value for α , we used the experimental value of 18×10^{-5} cm/watt-deg for pure iron, obtained by *Mendelssohn* and *Rosenberg* (1952).

From our experimental values of the residual electrical resistances of the steels, it was found that the αT^2 ($= w_i$) term amounted to less than 1% of β/T ($= \rho_o/L_o T = w_o$) near about 25°K, but rose to about 16% of w_o at about 70°K, for the 1287D steel. At lower temperatures, it rapidly became negligible compared to w_o . For the no. 3754 stainless steel, w_i was $\sim 18\%$ of w_o at 70°K, falling to less than 1% at about 40°K and becoming negligibly small at lower temperatures.

In the fig. IV, 3, of λ versus T , of the steels, the curves marked λ_e are thus the function

$$\lambda_e = 1/w_e = (\beta/T + \alpha T^2)^{-1} = (\rho_o/L_o T + 18 \times 10^{-5} T^2)^{-1} \quad (\text{IV, 1})$$

The values used for ρ_o for the steel rods no. 1287D, 3703, 1287I, 1797H and 3754 were respectively 9.3, 12.9, 27.7, 41.5, and 47.8 $\mu \Omega \text{cm}$.

Assuming that the electronic and lattice thermal conductivities add up together to give the total thermal conductivity, we can write, as we did in chapter II (equation II, 31)

$$\lambda = \lambda_e + \lambda_g$$

Knowing λ experimentally, and λ_e as indicated above, we obtained the values of λ_g at various temperatures.

Using the values of λ read off the λ versus T graphs, and the electrical resistivity ρ from the ρ versus T graphs, the *Wiedemann-Franz-Lorenz* parameter L ($= \rho/wT = \lambda\rho/T$) is calculated at different temperatures and plotted in fig. IV, 4.

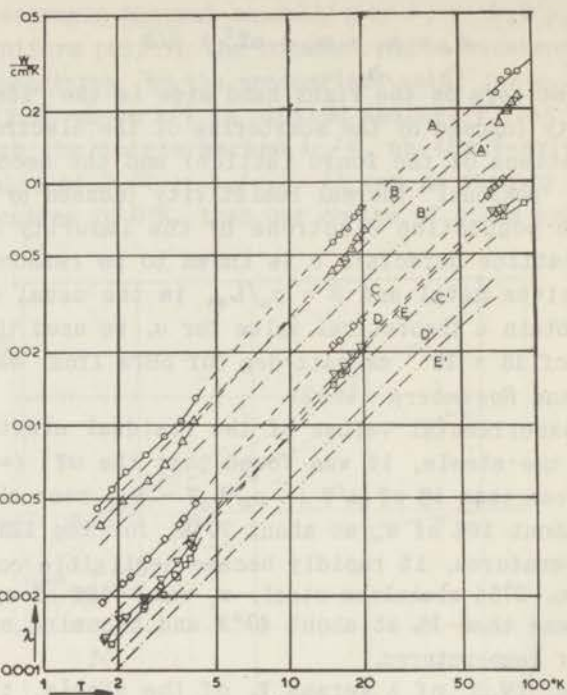


Figure IV, 3

The steels: λ and λ_e , both in watts/cm-deg, versus Temperature. \odot 1287D (curve A), \triangle 3703 (curve B), \diamond 1287I (curve C), ∇ 1798H (curve D), \square 3754 (curve E). A, B, C, D, and E are the λ -curves, and A', B', C', D' and E' are the λ_e -curves. (The data for the no. 3754 stainless steel, in the liquid Oxygen region, are taken from De Nobel, 1951.)

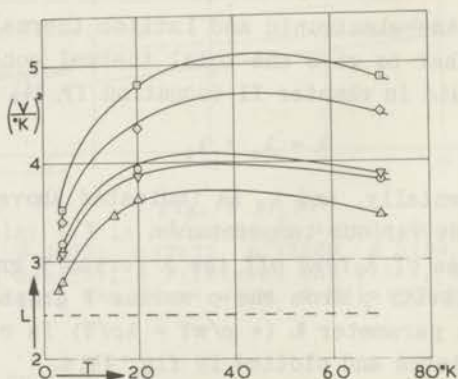


Figure IV, 4

The steels: L in (Volt/deg)², versus Temperature. \triangle 1287D, \odot 3703, ∇ 1287I, \diamond 1798H, \square 3754.

Table IV, 2
The steels: λ (in mW/cm-deg) against T°K.

No. 1287D		No. 3703		No. 1287I		No. 1798H		No. 3754	
T	λ	T	λ	T	λ	T	λ	T	λ
4.116	12.76	4.044	10.26	4.080	4.72	3.888	3.17	4.004	3.11
3.595	10.27	3.626	8.43	3.648	4.06	3.446	2.68	3.702	2.64
3.055	8.90	3.070	6.89	3.503	3.85	2.952	2.29	3.350	2.41
2.568	7.43	2.616	5.80	3.046	3.36	2.519	1.93	2.930	2.17
2.116	6.35	2.062	4.81	2.590	2.79	2.126	1.60	2.535	1.82
1.860	5.41	1.663	3.81	2.209	2.36	1.750	1.32		
1.614	4.53			2.045	2.22			3.884	2.80
		20.60 ⁰	63.8	1.690	1.85	3.937	3.34	3.434	2.35
19.98 ²	77.9	19.14 ³	58.6			2.516	1.91	3.026	1.99
19.39 ³	74.5	18.15 ⁰	52.5	19.83 ³	26.7	1.989	1.58	2.500	1.75
18.57 ³	71.5	18.13 ⁹	48.1	18.34 ⁶	25.1	1.718	1.30	1.843	1.25
17.52 ⁸	63.8	16.16 ⁵	45.9	16.12 ⁰	21.8				
16.17 ⁵	60.3	15.04 ²	42.2	15.08 ⁴	20.9	19.68 ⁸	20.6	19.83 ⁵	20.1
15.16 ⁸	56.1					18.31 ²	19.1	17.10 ⁶	16.8
		87.64	227	76.13	102.3	16.84 ¹	17.2	16.29 ⁴	16.0
87.70	286	82.92	211	73.62	96.9	15.19 ⁰	15.9	15.16 ⁹	14.6
80.36	289	80.05	195	70.39	93.9				
75.34	263	79.80	199	68.04	91.8	76.34	77.0	19.82 ⁰	20.8
71.49	232	73.76	175	65.93	86.1	73.52	74.9	18.68 ⁵	19.2
						71.12	73.5	17.08 ⁰	16.4
								16.41 ⁰	16.3
						71.18	73.7	15.31 ⁴	15.9
						68.32	74.6		
								92.8*	81.4*
								76.3*	71.4*

Data at liquid Oxygen temperatures for the stainless steel No. 3754 (marked *), are from *De Nobel* (1951).

§ 3. Discussion

The λ versus T curves:

The rather slow fall in λ on cooling certain metallic alloys to liquid Nitrogen temperatures, and a steeper fall at lower temperatures, first noticed in the measurements of *Lees* (1908) and of *Bremmer* and *De Haas* (1932, 1936) were found also in a wide

range of alloys by later experimenters in the field of low temperature thermal conductivities. We wish to draw attention to the behaviour of our λ versus T curves at liquid Helium temperatures, brought out more vividly in fig. IV,2, where λ/T is plotted against T. There is a marked hump in these curves for the steels no. 1287D and 3703, as in the case of the silver-base alloys. For the remaining three steels, the hump is not so well marked. It has been suggested in chapter III that this hump is associated probably with the lattice thermal conductivity.

The λ for the steel (containing 0.50-0.70%Mn, 0.4%C, 0.3%Si, 0.3%P and 0.03%S) reported by *Karweil and Schäfer* (1939) is close to that for our 1287D steel, at liquid Helium temperatures. At 3°K, they found $\lambda = 7.5$ mW/cm-deg, whereas we obtain 8.7 mW/cm-deg.

The values of λ given by *Wilkinson and Wilks* (1949) for a stainless steel specimen between 10 and 20°K are about 3/4 of the values obtained by us for the 3754 stainless steel specimen at the same temperatures.

For the steel Ae Ju2 (containing 16.05 Cr, 9.89 Ni, 0.66 Mn, 0.88 Si and 0.26 C), *Zlunitzin and Saveljev* (1939) reported $\lambda = 18.9$ mW/cm-deg at 18°K, which corresponds closely with the value 18.8 mW/cm-deg at 18°K, obtained by us for the 1798H Nickel-steel, whereas our stainless steel specimen No. 3754 gave 17.8 mW/cm-deg at 18°K.

Our results at Helium temperatures for the 1798H and 3754 steels correspond to those of *Schmeissner and Meissner* (1950) on Chroman B2Mo (an alloy containing, by weight, 61.4 Ni, 18.5 Cr, 14.5 Fe, 3 Mn, 2 Mo, and 0.6 Si). These authors give λ at 3.9°K as 2.6 mW/cm-deg, and their electrical resistivity at liquid Helium temperatures is more than twice that of our steels no. 1798H and 3754. The type 303 stainless steel (18 Cr, 9 Ni, 0.15 C) studied by *Estermann and Zimmermann* (1952) has at liquid Helium temperatures, a thermal resistivity 1.5 times as large as these, but at liquid Hydrogen temperatures, its thermal resistivity is similar to our no. 3754.

The values of the over-all thermal conductivity, as also of the lattice component reported by *Berman* (1951b) for a stainless steel specimen (18.9 Cr, 7.9 Ni, 1 Ti, 0.7 Si, 0.1 C) are close to the corresponding values obtained by us for the nos. 1798H and 3754 steels.

The lattice thermal conductivity:

Reference was made in chapter II to the various scattering mechanisms contributing to the lattice thermal resistivity and functioning as thermal resistances in series. Amongst them, the one dominating would be that with the highest contribution to the total resistivity; or, in other words, the one that tends to limit the conductivity to the lowest value. The w_g versus T curves for the steels measured by us show that no single simple power law is obeyed throughout the temperature regions. There are, however, narrow temperature regions between about 4 and 6°K where the lattice thermal resistivity seems closely proportional to T^{-2} . From these, one could make a rough estimate of the corresponding scattering coefficient. In chapter II, we had expressed w_g as

$$w_E = E/T^2 \quad (\text{II, 34})$$

when the dominant scattering mechanism is afforded by the conduction electrons. It appears therefore, that the scattering coefficient derived in this manner is E . The estimated values of E are 9850, 7000, 15000, 16200 and 16200 cm-deg³/watt, respectively for the five steel specimens, in the order of increasing foreign metal content. We wish to make it clear here, that our measurements do not cover the intervening region between the liquid Helium and liquid Hydrogen temperatures. By interpolation between the measured points, the values of λ at intermediate temperatures are obtained (fig. IV, 3) from which w_g is derived in the usual manner. The values thus obtained for E serve a useful purpose in giving us a rough idea of their magnitude. However, unless these are corroborated by some other method, we cannot give them much weight.

One could express the lattice thermal conductivity of the steels between 6 and 25°K, by a relation of the form

$$\lambda_g = \text{constant} \times T^n \quad (\text{IV, 2})$$

In the order of increasing foreign metal content, these relations are,

- i) $\lambda_g = 5.5 \times 10^{-4} \times T^{1.26}$,
- ii) $\lambda_g = 5.6 \times 10^{-4} \times T^{1.24}$,
- iii) $\lambda_g = 2.6 \times 10^{-4} \times T^{1.21}$,

$$\text{iv) } \lambda_g = 2.5 \times 10^{-4} \times T^{1.21},$$

$$\text{v) } \lambda_g = 2.2 \times 10^{-4} \times T^{1.26},$$

where λ_g is in watts/cm-deg. The power of T being less than 2 in these equations, suggests that in addition to the scattering by electrons, the phonons are scattered also by impurities, rather than by the mutual scattering of phonons, since the last-mentioned varies too rapidly with T to give a resultant λ_g of the type actually observed.

De Nobel (1951) concluded from his results at liquid Hydrogen temperatures that the over-all thermal conductivity for the steels is proportional to T^n where n lies between 1.07 and 1.47. Our results for λ_g give for n , the values 1.06, 1.04, 1.05, 1.09 and 1.11 respectively for the steels 1287D, 3703, 1287I, 1798H and 3754.

We add here, for purposes of comparison, the results obtained for cupro-nickel alloys. *Estermann* and *Zimmermann* (1952) found for a $\text{Cu}_{90}\text{Ni}_{10}$ alloy specimen, between 5 and 15°K, $\lambda_g = 0.39 T^2$ mW/cm-deg; while, using the thermal conductivity data of *Wilkinson* and *Wilks* (1949) and the electrical resistivity data from *Landolt* and *Bornsteins' Physikalisch-Chemische Tabellen*, (Verlag Julius Springer, Berlin, 1923, Hw, p.1054), they derived for the alloy $\text{Cu}_{70}\text{Ni}_{30}$, the approximate relation $\lambda_g = 0.11 T^2$ mW/cm-deg, correct near about 12°K. *Hulm* (1951) has reported for an annealed $\text{Cu}_{80}\text{Ni}_{20}$ specimen, $\lambda_g = 0.22 T^{2.0}$ mW/cm-deg, while theoretically for scattering of phonons by electrons, he expected $\lambda_g = 0.11 T^2$ mW/cm-deg. For the specimens measured by *Karweil* and *Schäfer* (1939), the following empirical relations were derived:

German-silver ($\text{Cu}_{64}\text{Ni}_{16}\text{Zn}_{20}$): $\lambda_g = 0.38 T^{2.0}$ mW/cm-deg.

Silver-bronze ($\text{Cu}_{46}\text{Ni}_{13}\text{Zn}_{41}$): $\lambda_g = 0.47 T^{1.5}$ mW/cm-deg.

Contracid ($\text{Ni}_{60}\text{Cr}_{15}\text{Fe}_{16}\text{Mo}_7$): $\lambda_g = 0.20 T^{1.4}$ mW/cm-deg.

The *Wiedemann-Franz-Lorenz* parameter:

Fig. IV,4 gives a plot of L against T , for the various steels measured by us. The values of L for the 1287D steel at the lowest temperatures closely correspond to those reported by *Karweil* and *Schäfer* (1939) for his steel specimen containing less than 1% impurity. At 3, 10, and 20°K, they obtain $L = 2.5, 3.3$ and 5.0 respectively, while we find for the 1287D steel, the values 2.6, 3.25 and 3.6 at the same temperatures.

The values obtained for the no. 3754 stainless steel are very

similar to those obtained by *Estermann and Zimmermann* (1952) for their stainless steel type 303. Both have a broad maximum with a nearly constant value of L , between 20 and 70°K, with just this difference that whereas L ranges between 4.8 and 5.1 in our no. 3754 stainless steel specimen (in that temperature interval), it is between 5.4 and 5.9 in their specimen.

The rise of the W - F - L parameter above the *Sommerfeld* value (2.45×10^{-8} volt²/deg²) is considered, in theory, to be an indication of appreciable lattice thermal conduction.

Variation of λ with foreign metal content:

Fig. IV, 5, shows the variation of thermal conductivity with percentage of foreign metal content. In the stainless steel no. 3754, since there are 18.80 atoms of Chromium and 8.10 of Nickel, we consider it roughly as having 27 atoms of foreign metal. In

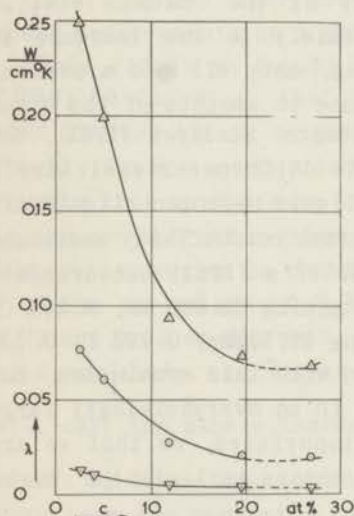


Figure IV, 5

The steels: λ in watts/cm-deg, versus percentage of foreign metal content "c".
 Δ 70°K, \circ 20°K, ∇ 4°K.

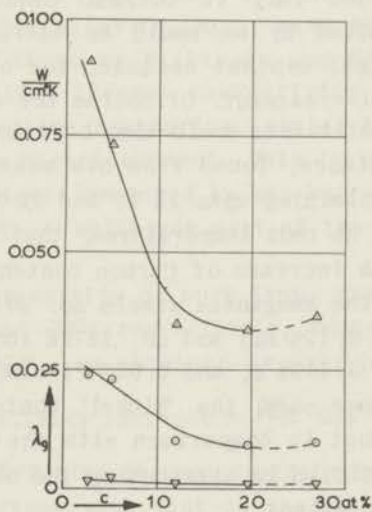


Figure IV, 6

The steels: λ_g in watts/cm-deg, versus percentage of foreign metal content, "c".
 Δ 70°K, \circ 20°K, ∇ 4°K.

the 1287D steel, there are 0.72 atoms of Manganese to 1.92 of Nickel, and we consider it as having 2.6 atoms of foreign metal. For the remaining three steels, the Manganese content is ignored. In the graphs of figs. IV, 5, IV, 6, and elsewhere, the portions of

the curves leading to 27% foreign metal content are shown dashed, indicating that we added up the number of Chromium and of Nickel atoms, irrespective of whether it is justified. With this reservation, we shall treat all the five as 'Nickel-steels'.

Three curves are shown in fig. IV,5, representative of the three low temperature regions, - liquid Nitrogen, Hydrogen and Helium. It is seen from these curves that the thermal conductivity falls with increasing impurity metal content, this fall being steeper, the higher the temperature. With further increase of impurity metal content, the thermal conductivity would probably rise again, as was found by *De Nobel* (1951). The extensive measurements of *De Nobel* on Nickel-steels containing 0 to 99.4 per cent of Nickel, showed that for the liquid air and liquid Hydrogen temperatures, the thermal conductivity diminishes with increasing Nickel content, reaching a minimum at about 26% Ni and rising thereafter.

The fall in thermal conductivity of the 'Nickel steels' studied by us could be attributed mainly to the increase in Nickel content because, for one thing, they all had a similar heat-treatment. Of course the difference in amounts of the other constituents could also have some influence. *Saveljev* (1941), for instance, found from his measurements on Chrome-Nickel steels (containing upto 1% Cr and 5% Ni) at liquid Hydrogen, liquid air and at room temperatures, that the thermal conductivity decreased with increase of Carbon content. *De Nobel's* (1951) measurements on the Manganese steels no. 1010 (containing 12.69% Mn, 1.27% C, and 0.12% Si) and no. 1379E (containing 12.95%Mn, 0.09% C, 0.12% Si, 0.103% S, and 0.05% P) also agreed with this conclusion. But in our case, the 'Nickel' content was in an overwhelmingly large amount in comparison with the other impurities, so that we are justified in attributing the observed change in λ , to the 'Nickel' content.

Even though the fall in λ with increase in 'Nickel' content is more marked in the 70°K curve, the percentual decrease in thermal conductivity, in passing from 2% Ni to 27% (Ni+Cr) is nearly the same whichever part of the low temperature region we might consider. The percentages referred to, are actually 72, 74 and 75 respectively at 70, 20 and 4°K.

The lattice thermal conductivity against impurity metal content, plotted in fig. IV,6, has the same general characteristics as the curves of Fig. IV,5. Both the series of curves show a linear fall in conductivity on increasing the Nickel content from

2 to 12%, and then they flatten out somewhat, exhibiting a minimum at about the same Nickel concentration. The percentage fall in λ_g in passing from 2 to 27% foreign metal content amounts to 60, 58, and 37 at the temperatures 70, 20 and 4°K respectively, while the corresponding fall in λ_e is about 80% whichever part of the low temperature region be considered. Thus the addition of the impurity has affected λ_e more than λ_g . This is understandable because at these temperatures, λ_e is limited considerably by impurity scattering, whereas in the case of λ_g , there are also other scattering mechanisms (besides impurity scattering) which are not much affected by the addition of impurity. Further the effect of impurity on λ_g is noticeable more at liquid Hydrogen temperatures and above rather than at liquid Helium temperatures. This is also understandable because at these higher ranges of the low temperature region, impurity scattering is very effective in limiting lattice thermal conduction.

Estermann and Zimmermann (1952) conclude from a comparison of their measurements on a Cupro-Nickel alloy $\text{Cu}_{90}\text{Ni}_{10}$, with those by *Hulm* (1951) on $\text{Cu}_{80}\text{Ni}_{20}$, and those by *Wilkinson and Wilks* (1949) on $\text{Cu}_{70}\text{Ni}_{30}$, that the lattice thermal conductivity λ_g , when limited mainly by phonon-electron scattering, varied in a roughly inverse proportion to the Nickel content. This is also roughly true in the case of the steels measured by us, but only in the concentration range 2-12% Ni, - whichever part of the low temperature region be considered.

Using the values of thermal resistivity of pure Iron, namely 1.72 and 0.52 cm-deg/watt, at 4 and 20°K respectively, reported by *Mendelssohn and Rosenberg* (1952), we obtained δw (which we will call the atomic thermal resistivity increase = $\frac{\Delta w}{c}$) for the steels at these temperatures. At 70°K, the thermal resistivity of pure iron was neglected in comparison with that of the alloys. Fig. IV, 7 gives a plot of δw against the amount of foreign metal, expressed in atomic percentage 'c'.

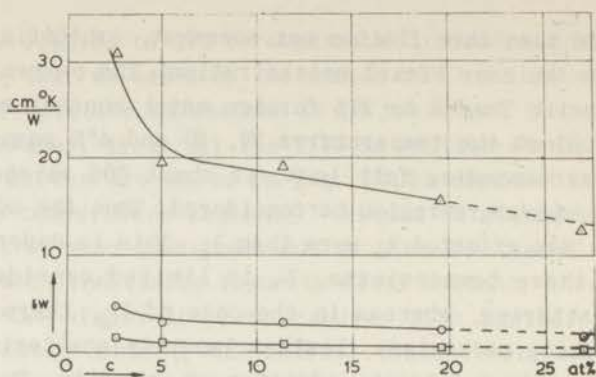


Figure IV, 7
The steels: Atomic thermal resistivity increase δw , in cm-deg/watt, versus percentage of foreign metal content, 'c'

The λ/T versus T curves:

Fig. IV, 2 gives the plots of λ/T (expressed in $\text{mW}/\text{cm-deg}^2$) versus T , of the steels measured by us. For purposes of comparison, we have also plotted measurements on steels by *Berman* (1951b), *Estermann* and *Zimmermann* (1952), *Karweil* and *Schäfer* (1939) and by *Wilkinson* and *Wilks* (1949). *Berman* has not given the actual values of λ in his paper: we have therefore read off the values of λ from the plotted points in the National Bureau of Standards circular 556, fig. 23. The rest of the above-mentioned investigators have given the values of λ at specified temperatures, which we have directly plotted. The measurements of *Wilkinson* and *Wilks* do not extend to liquid Helium temperatures. Those of *Karweil* and *Schäfer* and of *Estermann* and *Zimmermann* are rather scattered, so that a straight line had to be drawn for the entire region plotted. The measurements of *Berman* are very satisfactory: they show that the curve at liquid Helium temperatures is a straight line (indicating that the scattering of phonons by electrons is the dominant mechanism limiting lattice thermal conductivity) and the curve bends away from rectilinearity above about 6°K , indicating the onset of phonon-impurity scattering and a consequent reduction in lattice thermal conduction. This behaviour shown by *Berman's* curve, and by the curve of *White* and *Woods* (in fig. III, 2) is completely in accordance with theory and lends support to our method of analysis of the λ/T versus T curves, already described.

The phonon-impurity scattering in the steels can be seen to be

effective even at such low temperatures as 6°K. This, and the anomaly obtaining at liquid Helium temperatures proper, could possibly account for the fact that the proportionality of w_g with the inverse square of T (already referred to) was noticeable only in a very restricted temperature interval. The procedure for analysis of the λ/T versus T curves is just the same as for the Silver-base alloys. The values of λ_o/T and L_o/ρ_o here, fit nicely, and the anomaly is not very marked in the steels 1287I, 1798H and 3754. We draw attention to *Hulm's* (1951) measurements on $Cu_{80}Ni_{20}$, also plotted in fig. IV, 2. There seems to be an indication of an anomaly between 3 and 3.5°K. As a matter of fact, the two measured points of *Estermann* and *Zimmermann* in the liquid Helium region suggest that detailed measurements would probably have given a slight anomaly as in the case of our stainless steel no. 3754. The points of *Berman* at about 4.5 and 5.2°K are also suggestive. It appears therefore that in our discussion of the anomaly in chapter III, we over-simplified the picture, laying emphasis on 'suitably' diluted alloys. The actual causes are probably more complex and the phenomenon more general. It would need very careful and more measurements at liquid Helium temperatures in order to be able to discuss this anomaly more definitely.

The values of the phonon-electron scattering coefficient E for

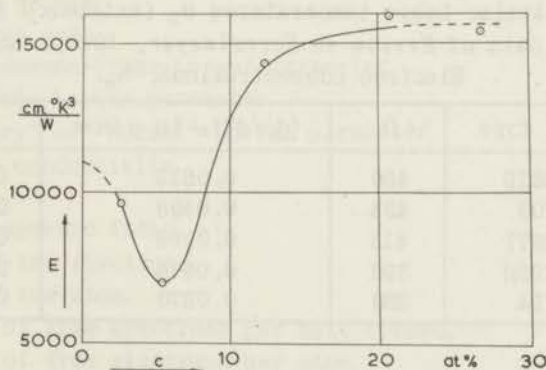


Figure IV, 8
The steels: Phonon-Electron scattering coefficient E , in $cm \cdot deg^3/watt$, versus percentage of foreign metal content, 'c.'

the steels, obtained from the λ/T versus T curves are 9620, 7000, 14300, 15900 and 15400, in the order of increasing foreign metal

content. Fig. IV,8 gives a plot of E (in $\text{cm-deg}^3/\text{watt}$) against percentage 'c' of the foreign metal content. Extrapolation of the curve to $c = 0$, gives $E \sim 11000$ for pure Iron. As we did in the case of pure Silver, we can evaluate N_a for pure Iron, assuming the *Makinson* coupling scheme and the value of $\alpha = 1.8 \times 10^{-4}$ (*Mendelssohn and Rosenberg, 1952*). We also take $\theta_D = 460^\circ\text{K}$ (*Keesom and Kurrelmeyer 1939*) for pure Iron. We have then $\lambda_g = T^2/11000$, and $\lambda_i = 1/\alpha T^2$, so that

$$\lambda_g/\lambda_i = 313 (T/\theta)^4 N_a^{-4/3}.$$

We thus obtain $N \sim 0.5$.

As suggested in equation (II,40), we can use the $(d\rho/dT)_\infty$ of the alloys, for a similar calculation. We have the electrical resistivities of the steels at the ice-point and the steam-point, from which $(d\rho/dT)_\infty$ is obtained. Using the formula

$$N_a^2 = \frac{4.93 E}{\theta^2} \cdot \frac{L}{(d\rho/dT)_\infty},$$

we can calculate N_a for the various steels (see Table IV,3). We can then estimate N_a for pure Iron to be of the order of 0.3. This value and the value obtained above for pure Iron, are not quite equal, because in this case we are comparing low tempera-

Table IV,3

The steels: Debye temperatures θ_D (estimated from the data of *Keesom en Kurrelmeyer, 1940*), and Electron concentrations, N_a .

Steel type	D	$(d\rho/dT)_\infty$ in $\mu\Omega\text{cm}$	N_a
1287D	450	0.0612	0.31
3703	435	0.0598	0.27
1287I	415	0.0786	0.36
1798H	390	0.0678	0.43
3754	380	0.0870	0.38

ture lattice thermal conductivity with λ_i at high temperatures. Yet, the order of the value derived, is quite satisfactory.

List of important symbols used

a	Lattice constant.
<u>b</u>	Fundamental vector of reciprocal lattice.
c_v	Specific heat per unit volume.
C	Constant of interaction between electrons and phonons.
C_L	Constant of interaction between electrons and longitudinal phonons
-e	Charge of the electron.
ϵ	Energy of electron. (In chapter I, § 1, $\epsilon = T - \tau$).
E	Coefficient of phonon scattering by electrons.
ζ	Fermi energy.
θ, θ_D	Debye characteristic temperature.
f	Distribution function.
f_0	Distribution function at equilibrium.
h	Planck's constant.
\hbar	$h/2\pi$.
H	Magnetic field-strength.
<u>k</u>	Wave vector of electronic wave function.
k	Wave number.
k	Boltzmann constant.
$^{\circ}\text{K}$	Degrees Kelvin.
l	Mean free path.
L	The Wiedemann-Franz-Lorenz parameter.
L_e	Electronic Lorenz parameter.
L_o	"Ordinary" or "Normal" Lorenz parameter.
λ	Thermal conductivity.
λ_i	λ_{ideal} .
λ_H	λ in magnetic field.
m	Mass of the electron.
M	Mass of the atom.
n	Number of free electrons per unit volume.
N_a	Number of free electrons per atom.
ν	Frequency.
ω	Angular frequency = $2\pi\nu$.
<u>q</u>	Wave vector of lattice vibrations.
ρ	Electrical resistivity.
ρ_i	ρ_{ideal} .
ρ_o	$\rho_{residual}$.

List of references

- Babbitt, J.D. and Mendelssohn, K., 1935, *Phil. Mag.* **20**, 1025.
- Berman, R., 1951a, *Proc. Roy. Soc. (London)*, A **208**, 90.
1951b, *Phil. Mag.* **42**, 642.
1953, *Advances in Physics*, **2**, 103.
- Berman, R., et al., 1953, *Proc. Roy. Soc. (London)*, A **220**, 172.
- Bethe, H., 1933, in *Handbuch d. Physik.*, **24**, 2nd ed., part 2.
- Biermasz, Th., 1938, Thesis, Leiden.
- Blackman, M., 1951, *Proc. Phys. Soc. (London)*, A **64**, 681.
- Bloch, F., 1928, *Z. Physik.* **52**, 555; 1930, *Z. Physik.*, **59**, 208.
- Bohm, D., and Pines, D., 1951, *Phys. Rev.* **82**, 625; 1952, *Phys. Rev.* **85**, 338; 1953, *Phys. Rev.* **92**, 609; 1954, *Phys. Rev.* **92**, 626.
- Bremmer, H., 1934, Thesis, Leiden.
- Bremmer, H. and de Haas, W.J., 1932, *Proc. Roy. Acad. Amsterdam*, **35**, 323, *Comm. Kamerlingh Onnes Lab. Leiden*, No. 220; 1936, *Physica*, ('s-Grav.), **3**, 692.
- Brown, A., Zemansky, M.W., and Boorse, H.A., 1951, *Phys. Rev.* **84**, 1050.
- Casimir, H.B.G., 1938, *Physica*, **5**, 495, *Leiden. Comm. Suppl.* No. 85b.
- Cath, P.G., 1918, *Proc. Roy. Acad. Amst.* **21**, 656; *Leiden. Comm.* No. 152d.
- Clement, J.R. and Quinnell, E.H., 1952, *Rev. Sc. Inst.* **23**, 213.
- Debye, P., 1914, *Vortrage über die Kinetische Theorie der Materie und der Elektrizität* - Teubner, Leipzig.
- De Haas, W.J. and Biermasz, Th., 1935, *Physica*, **2**, 673, *Leiden. Comm.* No. 236e; 1937, *Physica*, **4**, 752, *Leiden. Comm.* No. 249a.
- De Haas, W.J., and Bremmer, H., 1934, *Proc. Roy. Acad. Amst.* **34**, 325, *Leiden. Comm.* No. 214d.
- De Haas, W.J., and Hadfield, R.A., 1933, *Phil. Trans. Roy. Soc. (London)* A **232**, 297.
- De Nobel, J., 1951, *Physica*, **17**, 551; *Comm.* 285b.
1954, Thesis, Leiden.
- De Nobel, J. and Chari, M.S.R., 1955, *Proc. Int. Conf. Low Temp. Physics*, Paris.
- Dewar, J. and Hadfield, R.A., 1904, *Proc. Roy. Soc. (London)* A **74**, 326.

- Estermann, I. and Zimmermann, J.E., 1952, *J. Appl. Phys.* **23**, 578.
- Fröhlich, H., 1936, *Elektronen Theorie der Metalle*, Springer, Berlin.
- Gerritsen, A.N., 1953, *Physica*, **19**, 61; Comm. 291c.
- Gerritsen, A.N., 1955, *Proc. Int. Conf. Low Temp. Physics*, Paris.
- Gerritsen, A.N. and Korryng, J., 1951, *Phys. Rev.* **84**, 604.
- Gerritsen, A.N. and Linde, J.O., 1951a, *Physica*, **17**, 573, Comm. 285c; 1951b, *Physica*, **17**, 584, Comm. 285d; 1952, *Physica*, **18**, 877, Comm. 290d.
- Grüneisen, E., 1900, *Ann. Physik.*, **3**, 43.
- Hadfield, R. A., Woltjer, H.R., and Onnes, K., 1921, *Proc. Roy. Soc. (London)*, **A 99**, 174; Comm. 155.
- Hartree, D.R., 1928, *Proc. Camb. Phil. Soc.*, **24**, 89.
- Heitler, W., and London, F., 1927, *Z. Physik.* **44**, 455.
- Howling, D.H., et al., 1955, *Proc. Roy. Soc. (London)* **A 229**, 86.
- Hulm, J.K., 1951, *Proc. Phys. Soc. (London)* **A 64**, 207.
1950, *Proc. Roy. Soc. (London)* **A 204**, 98.
- Jaeger, W. and Diesselhorst, H., 1900, *Wiss. Abhand. Phys. Tech. Reichsanstalt*, **3**, 269.
- Karweil, J. and Schäfer, K., 1939, *Ann. Physik.*, **36**, 567.
- Keesom, W.H., 1934, *J. Phys. Rad.* **5**, 373; 1936, *Comm. Suppl.* 80a.
- Keesom, W.H., Bijl, A. and Miss van der Horst, H., 1931, *Proc. Roy. Acad. Amst.* **34**, 1223; Comm. 217a.
- Keesom, W.H. and Kurrelmeyer, B., 1939, *Physica*, **6**, 633, Comm. 257a; 1940, *Physica*, **7**, 1003, Comm. 260d.
- Keesom, W.H. and van den Ende, J.N., 1929, *Proc. Roy. Acad. Amst.* **32**, 1171, Comm. 203c.
- Kemp, W.R.G., et al., 1954, *Proc. Phys. Soc. (London)* **A 67**, 728; 1956, *Proc. Roy. Soc. (London)* **A 233**, 480.
- Klemens, P.G., 1951, *Proc. Roy. Soc. (London)* **A 208**, 108.
1954a, *Aust. J. Phys.* **7**, 57.
1954b, *Aust. J. Phys.* **7**, 64.
1954c, *Aust. J. Phys.* **7**, 70.
1955, *Proc. Phys. Soc. (London)* **A 68**, 1113.
1956, *Handbuch der Physik.*, Vol. XIV, (Springer Verlag).
- Kohler, M., 1948, *Z. Phys.* **124**, 772; 1949, *Z. Phys.* **125**, 679.
- Königsberger, J., 1907, *Phys. Zs.* **8**, 237.
- Korryng, J. and Gerritsen, A.N., 1953, *Physica*, **19**, 457, Comm. Suppl. 106.
- Kroll, W., 1933, *Z. Phys.* **80**, 50 and **81**, 425.
- Kronig, R. and Korryng, J., 1943, *Physica*, **10**, 406; Kronig., 1949, *Physica*, **15**, 667.

- Lees, Ch., 1908, *Phil. Trans. Roy. Soc. (London) A* **208**, 381.
- Linde, J.O., 1939, Thesis, Stockholm; 1948, *Arkiv. Mat, Astr. Fysik.* **36A**, No. 10.
- Makinson, R.E.B., 1938, *Proc. Camb. Phil. Soc.* **34**, 474.
- Matthiessen, A. and Vogt, C., 1864, *Ann. Physik. Chemie*, **122**, 19.
- Meissner, W., 1914, *Verh. d. D. Phys. Ges.* **16**, 262.
- Mendelssohn, K., and Rosenberg, H.M., 1952, *Proc. Phys. Soc. (London) A* **309**, 388.
- Norbury, A.L., 1921, *Trans. Farad. Soc. (London)* **16**, 570; Norbury, A.L. and Kuwada, K., 1927, *Phil. Mag.* **4**, 1338.
- Peierls, R.E., 1929, *Ann. Physik.* **3**, 1055; 1935, *Ann. Inst. Poincare*, **5**, 177.
- Pomeranchuk, I., 1941a, *J. Phys. USSR*, **4**, 259; 1941b, *Phys. Rev.* **60**, 820; 1942, *J. Phys. USSR*, **6**, 237.
- Powers, R.B., et al., 1951, TR 264+7, Cryogenics Lab., Ohio State University.
- Rosenberg, H.M., 1954a, National Bureau of Standards, Circular 556, p. 22.
- Saveljev, I., 1941, *J. Phys. USSR*, **4**, 383.
- Schmeissner, F., and Meissner, H., 1950, *Z. angew. Phys.* **2**, 423.
- Schott, R., 1916, *Verh. d. D. Phys. Ges.* **18**, 27.
- Sladek, R.J., 1955, *Phys. Rev.* **97**, 902.
- Sondheimer, E.H., 1950, *Proc. Roy. Soc. (London) A* **203**, 75; 1952, *Proc. Phys. Soc. (London) A* **65**, 562.
- Van Dijk, H. and Durieux, M., 1955, *Proc. Int. Conf. Low Temp. Physics, Paris*.
- Wexler, A., 1951, *J. Appl. Phys.* **22**, 1463.
- White, G.K., 1953a, *Aust. J. Phys.* **6**, 397.
1953b, *Proc. Phys. Soc. (London) A* **66**, 844.
1953c, *Proc. Phys. Soc. (London) A* **66**, 559.
- White, G.K. and Woods, S.B., 1954, *Phil. Mag.* **45**, 1343.
1955, *Canad. J. Phys.* **33**, 58.
- Wilkinson, K.R. and Wilks, J., 1949, *J. Sc. Inst.* **26**, 19.
- Wilson, A.H., 1937, *Proc. Camb. Phil. Soc.* **33**, 371.
- Worley, R.D. et al., 1954, *Phys. Rev.* **93**, 45.
- Zlunitzin, S. and Saveljev, I., 1939, *J. Tech. Phys. USSR*, **9**, 805.

General references:

1. Wilson, A.H., *Theory of Metals*: Camb. Univ. Press (1953).
2. Slater, J.C., *Modern Physics*, McGraw Hill Book Coy, 1955.
3. Seitz, F. and Turnbull, D., *Solid State Physics*, vol I, Academic Press Inc. New York, 1955.

4. Klemens, P.G., Article on 'thermal conductivity of solids at low temperatures' in Handbuch der Physik, Vol XIV. (Springer-Verlag).
5. Burton, E.F., Grayson-Smith, H., and Wilhelm, J.O., Phenomena at the temperature of liquid Helium (Reinhold publishing corporation, New York).
6. Olsen, J.L., and Rosenberg, H.M., Review article on 'thermal conductivity of metals at low temperatures' in Advances in Physics, 1953.
7. Powell, R.L., and Blanpied, W.A., 'Thermal conductivity of metals and alloys': National Bureau of Standards, U.S.A., Circular No. 556 (1954).

Samenvatting

(Summary in Dutch)

Warmtegeleiding in metallieke stoffen vindt, zoals bekend is, plaats zowel door middel van electronen als door roostertrillingen (de zogenaamde Debye-golven of phononen). De electronengeleiding wordt beperkt door de verstrooiing van electronen door 1) thermische roostertrillingen en 2) onzuiverheden (òf van chemische òf van natuurkundige aard). Roostergeleiding wordt beperkt door de verstrooiing van phononen door 1) kristal- en korrelbegrenzungen, 2) vrije electronen, 3) onzuiverheden en kleine roosterdefecten ('interstitials', vacatures, dislocaties, enz.) en 4) de andere phononen.

De theorie heeft in algemene zin de temperatuurafhankelijkheid van de weerstand, veroorzaakt door deze verschillende verstrooiingsmechanismen, kunnen voorspellen, maar veel experimentele gegevens zullen nog nodig zijn, voordat men verdere vooruitgang op dit gebied zal kunnen maken. De belangrijkheid van dergelijk onderzoek bij lage temperatuur wordt duidelijk, wanneer men overweegt, dat bij gewone temperaturen de invloed van de thermische trillingen die van alle andere verstrooiingsprocessen overschaduwet.

Het streven is steeds geweest om metingen te doen aan zuivere metalen (waarin warmtegeleiding door electronen overweegt) of aan dielectrische vaste stoffen (waarin alleen roostergeleiding optreedt). De weinige metingen aan legeringen tot nu toe gedaan, hadden betrekking op 'geconcentreerde' legeringen (d. w. z. die een hoog percentage van opgeloste atomen bevatten). Metingen van warmtegeleiding in verdunde legeringen (waaraan niet veel aandacht is besteed) en in staalsoorten vormen het onderwerp van dit proefschrift.

Wij beginnen in hoofdstuk I met een beschrijving van het principe van de gebruikte methode en van de toestellen. Details over de vervaardiging van weerstandthermometers, de wijze van calibratie en hun gedrag, worden beschreven. Een overzicht van de foutenbronnen en de bereikte nauwkeurigheid is ook gegeven.

Hoofdstuk II bevat de theoretische achtergrond, beginnend met een algemeen overzicht van de theorieën van de vaste toestand, in

het bijzonder in verband met metalen. Slechts terloops worden theorieën over de wisselwerking van electronen vermeld. Warmtegeleiding in dielectrische vaste stoffen wordt besproken in § 2. Daarin vindt men een overzicht van het Debye (continuum) model en van de bijdragen van Peierls, Pomeranchuk, Casimir en Klemens aan de beschouwingen over de verschillende mechanismen van phonon-verstrooiing en hun theoretische temperatuurafhankelijkheid. Warmtegeleiding in metalen en legeringen wordt besproken in § 3 en § 4, - het aandeel van de electronen in de warmtegeleiding in § 3 en dat van het rooster in § 4.

In hoofdstuk III delen wij uitkomsten van de metingen van elektrische en warmteweerstanden van verdunde zilverlegeringen mede. Drie van deze legeringen bevatten mangaan als opgelost metaal en de vierde bevatte indium. In de krommen van λ/T tegen T werd een maximum bij ongeveer 12°K voor deze reeks legeringen gevonden. Aandacht wordt besteed aan de anomalie in de warmtegeleiding bij temperaturen van vloeibaar helium, zoals in de $\lambda - T$ krommen is te zien en meer tot uiting is gebracht in de $\lambda/T - T$ en de $\lambda_g - T$ krommen. Omdat sterke magnetische velden de algemene vorm van de krommen niet belangrijk schijnen te wijzigen, is verondersteld, dat deze anomalie waarschijnlijk afkomstig is van de warmtegeleiding door het rooster.

De resultaten aan staalsoorten in hoofdstuk IV gegeven tonen een dergelijke anomalie bij de temperaturen van vloeibaar helium. Het schijnt daarom, dat deze anomale roostergeleiding bij lage temperaturen een zeker algemeen verschijnsel is. Verder leidt de vorm van de $\lambda - T$ krommen ertoe deze anomalie toe te schrijven aan een extra bijdrage tot de roostergeleiding. Men kan een analogie trekken tussen dit geval en de zogenaamde 'longitudinale' geleiding in kwartsglas, door Wilkinson en Wilks en door Berman waargenomen en theoretisch beschouwd door Klemens. De experimentele resultaten bij temperaturen van vloeibaar helium zijn, ondanks de aanwezigheid van de anomalie, zo goed mogelijk geanalyseerd. Daaruit kan men een waarde van de coëfficiënt E van de phonon-electronverstrooiing berekenen.

Stellingen

1. Van de verschillende modellen voor intermoleculaire potentia-
len, die kunnen worden aangepast aan de metingen van de tweede
viriaalcoëfficiënt in de toestandsvergelijking van eenvoudige
(niet polaire) moleculen, is bekend dat de potentiaalputten
min of meer gelijke oppervlakken hebben. Het is mogelijk dit
gedrag af te leiden van de wiskundige uitdrukking voor de
(tweede) viriaal-coëfficiënt (rekening houdende met de steil-
heid van de kanten van de potentiaalput).
2. Metingen over de anisotropie van gammastraling van gerichte
kernen zouden van nut zijn voor het onderzoek betreffende de
verdeling van de temperatuur in adiabatisch gedemagnetiseerde
zouten.
3. Metingen over het warmtegeleidingsvermogen, waarbij gebruik
wordt gemaakt van koolweerstand als thermometers en de gehe-
le staaft wordt opgewarmd ten opzichte van het bad, moeten niet
volkomen betrouwbaar worden geacht.
4. Dat leken in dezelfde mate zullen kunnen bijdragen tot de ont-
wikkeling van de natuurwetenschappen (en van natuurkunde in
het bijzonder), zoals in het verleden het geval is geweest, is
aan twijfel onderhevig.
5. Het zou aanbeveling verdienen de Gregoriaanse kalender, die
thans in gebruik is, te vervangen door een vaste, uniforme
kalender voor de gehele wereld.
6. Het is van belang het warmtegeleidingsvermogen bij lage tempe-
raturen te bepalen van verschillende staven van een diëlectri-
sche vaste stof, die een verschillende mozaïkstructuur bezit-
ten.
7. Indigo werd (door Newton) ingevoegd in de reeks van kleuren in
het spectrum om een betrekking te vinden tussen het spectrum
en de toonschaal. Aangezien de poging is mislukt, heeft het
geen zin indigo te handhaven als een fundamentele kleur tussen
violet en blauw.

(Zie b.v. 'Light and Colour' van R.A. Houston, Longmans
Green Co, London, 1923.)

8. Teneinde het aantal verkeersongevallen te verminderen dient men bij het maken van plannen voor stedenbouw langzaam en snelverkeer streng gescheiden te houden.
9. Om het talent voor tafeltennis in een land te ontwikkelen zou men het systeem moeten volgen van competities in verschillende klassen tussen de clubs, zoals dat b.v. in Nederland gebeurt.
10. Bij de metingen van het warmtegeleidingsvermogen van stoffen, die geen zeer goede geleiders zijn, is het noodzakelijk dat in de meetruimte om de staaf een vacuum wordt gehandhaafd van minstens 10^{-6} mm kwikdruk.

(Zie, b.v., W.R.G.Kemp et al, 1956, Proc. Roy. Soc. London, A 233, 450.)

